

VERTICAL CHANGES IN SHORELINE MORPHOLOGY AT INTRA-PARSEQUENCE SCALE

Manuel F. Isla ¹, Mariano N. Ramirez ¹, Ernesto Schwarz ¹, Gonzalo D. Veiga ¹

¹ Centro de Investigaciones Geológicas (Universidad Nacional de La Plata-CONICET).
Diagonal 113 #275 B1904DPK, La Plata, Argentina.

ARTICLE INFO

Article history

Received January 3, 2020

Accepted February 25, 2020

Available online February 25, 2020

Handling Editor

Sebastian Richiano

Keywords

intra-parasequence stratigraphy

barred shorelines

non-barred shorelines

Pilmatué Member

Neuquén Basin

ABSTRACT

It is commonly assumed in the high-resolution sequence stratigraphic analysis of shallow-marine deposits (e.g., deltaic and shoreface settings) that the depositional conditions of the system remain relatively constant during the transit of a shoreline that would eventually produce a single parasequence. However, based on the detailed sedimentary and architectural analysis of upper-shoreface and foreshore strata of two Early Cretaceous shoreface-shelf parasequences (Neuquén Basin, Argentina), it was possible to document a vertical change through the stratigraphy from deposits representing wave-dominated barred shorelines to deposits interpreted as representing a non-barred morphology. The presence of a well-defined limit between trough cross-bedded sandstones in the upper shoreface and planar laminated sandstones in the foreshore (and the presence of a surf diastem) characterize the development of barred shoreline conditions. Instead, planar lamination is ubiquitous within non-barred deposits, where trough cross-bedding is restricted to the bottomsets of the large-scale inclined beds that characterize this architectural style. Thickness, sediment composition and reconstructed shoreline trajectory also seemingly change vertically within the investigated parasequences. Collectively, these pieces of evidence suggest that the vertical transition from barred to non-barred deposits at this intra-parasequence scale could be related to wave-climate variations and the sequence-stratigraphic context. Specifically, changes in the prevailing wave behavior from dissipative to reflective conditions could be a feasible explanation for the morphological transformation of coastal systems through tens of thousands to hundreds of thousands years.

INTRODUCTION

Parasequences have been originally defined as shallowing-upward units limited by regional-scale flooding surfaces (Van Wagoner *et al.*, 1990), and which represents the progradation of a single/individual shallow-marine systems (delta-front and/or shoreface deposits; Table 1). Despite the great advances made in their knowledge, there are still big debates related to their controlling factors, time

span and their bounding surfaces (Zecchin and Catuneanu, 2013; Burgess *et al.*, 2016; Hampson, 2016; Muto *et al.*, 2016; Ridente, 2016; Zecchin *et al.*, 2017; Catuneanu, 2019). On the contrary, the temporal variability of the depositional systems as they prograde to form the parasequence has been less explored by sequence stratigraphers and it has been typically assumed that the configuration of the given shallow-marine system remains relatively constant (Van Wagoner *et al.*, 1988, 1990; Posamentier and

Author/s	Litostratigraphic unit, Locality	Sedimentary system	Parasequences
Pattison (1995); Hampson (2000); Hampson and Howell (2005); Sech <i>et al.</i> (2009)	Kenilworth Mb, Blackhawk Fm, Book Cliffs, Utah, USA	Wave-dominated shoreface-shelf (barred nearshore)	PS2; PS3; PS4 (K4); PS7 (Price River); PS8 (Battleship Butte)
Forzoni <i>et al.</i> (2015)	Panther Tongue Mb, Star Point Fm, Wasatch Plateau Utah, USA	Wave-dominated shoreface-shelf (barred nearshore) to fluvial-dominated delta	Ksp 040
Graham <i>et al.</i> (2015)	Ferron Sandstone Mb, Mancos Shale Fm, East-central Utah, USA	Fluvial-dominated delta	PSS1 to PSS8
Charvin <i>et al.</i> (2010); Hampson (2016)	Aberdeen Mb., Blackhawk Fm, Book Cliffs, Utah, USA	Wave-dominated shoreface-shelf (barred nearshore) to fluvial-dominated delta	Ab1; Ab2
Somme <i>et al.</i> (2008)	Sunnyside Mb. Blackhawk Fm, Book Cliffs, Utah, USA	Wave-dominated delta	S2; S3
Schwarz <i>et al.</i> (2018)	Pilmatué Mb., Agrio Fm, Neuquén, Argentina	Wave-dominated shoreface-shelf (barred nearshore)	PS240; PS360; PS380; PS500
Berton <i>et al.</i> (2019)	Quaternary deposits Praia de Leste, Brazil	Barrier/coastal plain	Pleistocene and Holocene parasequences
Longhitano and Steel (2017)	O'Brien Springs Sandstone Mb, Haystack Mountain Fm, Wyoming, USA	Tide-dominated delta	<i>Not defined</i>
Amorosi <i>et al.</i> (2017); Bruno <i>et al.</i> (2017)	Holocene, Po coastal plain, Italy	Floodplain and swamp	PS1
		Wave-dominated delta	PS2 to PS8
Rodriguez <i>et al.</i> (2005)	Holocene, Trinity River, Texas, USA	Estuary	<i>Not defined</i>
Gingras <i>et al.</i> (2002)	Pebas Fm, Amazon River, Perú	Marginal marine (lagoonal)	A, B and C
Pellegrini <i>et al.</i> (2017)	Quaternary deposits, Po River, Italy	Shelf-edge complex	Clinothems type A, B and C
Ainsworth <i>et al.</i> (2008)	Upper Plover Fm, Bonaparte Basin, Australia	Fluvial- or- wave-dominated delta	HST1a, HST1b, HST2a...

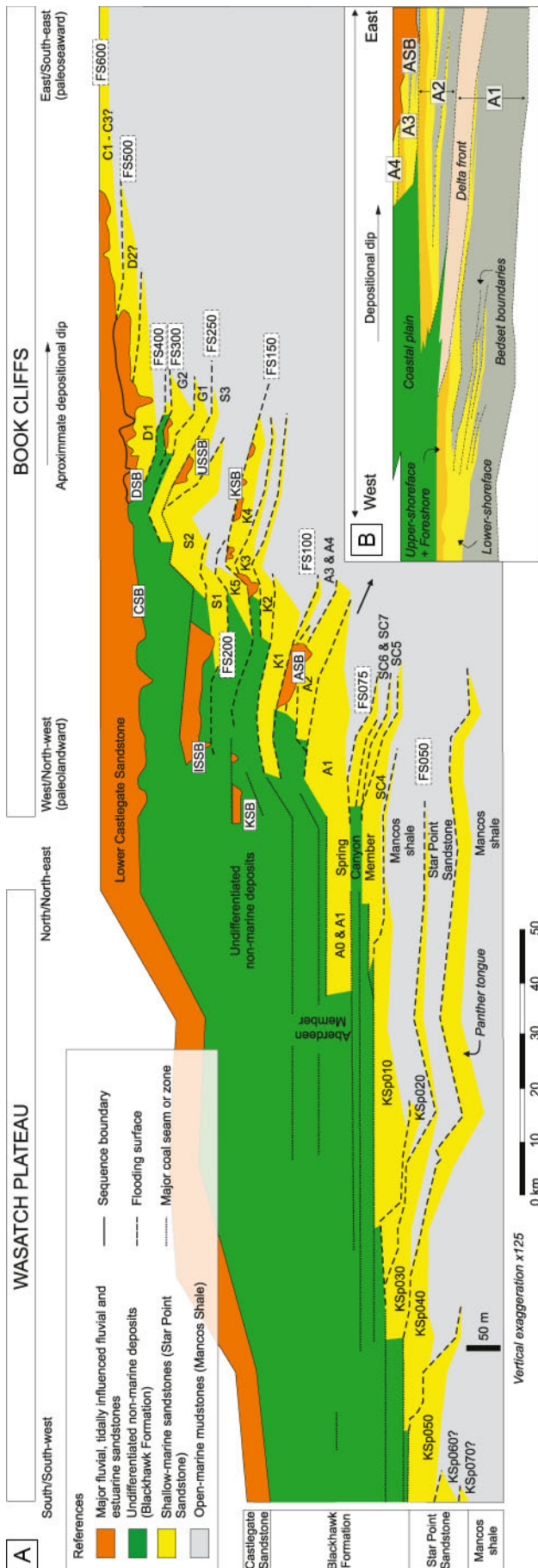
Table 1. Previous high-resolution studies of the stratigraphic architecture of parasequences.

Allen, 1999). This has been the case for most of the examples reported in the literature, for example in many outcropping parasequences in the Cretaceous of the Book Cliffs (Utah, USA) (Fig. 1a). Infrequently, the lateral and vertical juxtaposition of shoreface and delta front strata/bedsets has been documented within a single parasequence (e.g. Charvin *et al.*, 2010; Fig 1b), and was attributed to the spatial-related co-existence of delta-front settings and wave-dominated shoreline systems. The apparent low variability of shallow-marine strata at intra-parasequence scale lead to classify these high-frequency units as deltaic, shoreface (linear coasts) or deltaic-shoreface based on the interpreted formative shoreline (Colombera and Mountney, 2020).

The record of wave-dominated clastic shorelines typically consists in deposits of the upper-shoreface and foreshore settings within the shoreface-shelf systems, which are highly susceptible to changes in

wave climate (Clifton, 2006). Their morphological configuration is extremely dynamic and may vary from barred to non-barred conditions in short time spans (Davidson-Arnott, 2010). These different configurations are related to: (i) the presence or complete absence of nearshore bars separated by longshore troughs, which in turn are mostly linked to the gradient of coastal profiles and (ii) the dissipative versus reflective mechanisms developed under those gradients (Aagaard *et al.*, 2013). Recent studies have demonstrated that the seaward migration (progradation) of barred and non-barred shorelines produce different architectural styles in the stratigraphic record (Isla, 2019). However, this short-term variability of shallow-marine systems during the progradation of an individual shoreline, particularly for wave-dominated shoreface-shorelines systems, has not been documented.

Parasequences comprising wave-dominated



shoreface-shelf deposits are ubiquitous in the Early Cretaceous Pilmatué Member of the Agrio Formation in the Central Neuquén Basin (Argentina). The aims of this work are two-fold: 1) to describe and interpret barred and non-barred architectural elements and their vertical juxtaposition within two parasequences, 2) to discuss the possible processes controlling these temporal changes within the progradation of a wave-dominated clastic shoreline.

GEOLOGIC AND STRATIGRAPHIC BACKGROUND

The Neuquén Basin is located in the west-central sector of Argentina (Fig. 2a) and comprises a continuous stratigraphic record from the Late Triassic to the Early Cenozoic (Vergani *et al.*, 1995; Howell *et al.*, 2005). To the west, it is limited by the Andean Volcanic Arc, whereas the Sierra Pintada System and the Northpatagonian Massif constitute the northeast and southeast borders, respectively (Fig. 2a). It is characterized by a complex history of tectono-stratigraphic evolution which involves an initial rift phase during the Late Permian to the Early Triassic (Howell *et al.*, 2005) which lasted until the Early Jurassic to Middle Jurassic, when a post-rift phase started and the basin was reconfigured as a unified back-arc basin. During this phase, sedimentation was governed by eustatic changes and the uplift of the magmatic arc, as both conditioned the connection with the proto-Pacific Ocean, and thus controlled the sea level in the semi-enclosed basin (Legarreta and Uliana, 1991). Since the Late Cretaceous the basin has behaved as a foreland basin (Howell *et al.*, 2005).

The Pilmatué Member is the lowermost unit contained in the Agrio Formation and was accumulated between the late Valanginian and

Figure 1. a) Stratigraphic framework of the Cretaceous record in the Book Cliffs outcrop belt (Utah, USA). Stacked parasequences dipping approximately to the south-east, mainly consist in shoreface-shelf sandstone tongues. Updip, shallow-marine deposits pass to non-marine deposits (modified from Hampson *et al.*, 2012). Deltaic-shoreface parasequences are in bold. b) Within the Aberdeen Member, one of the parasequences (A1), record the interaction between shoreface and delta front deposits at intra-parasequence scale (modified from Charvin *et al.*, 2010; Hampson, 2016).

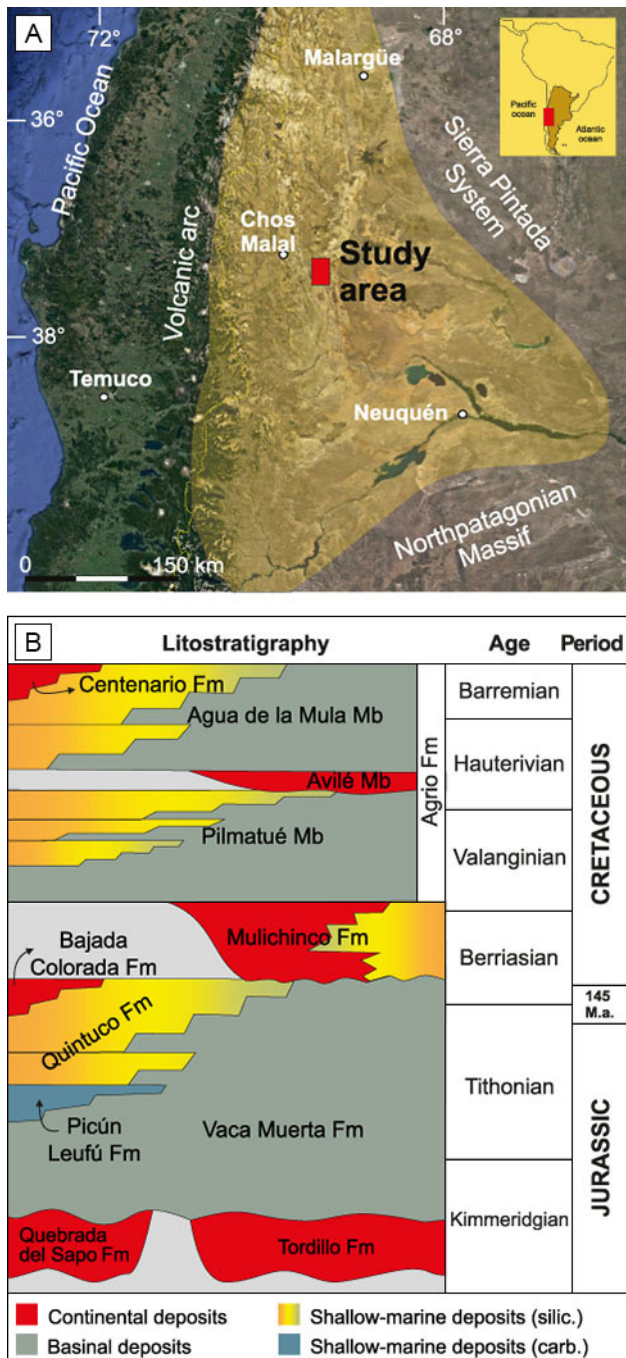


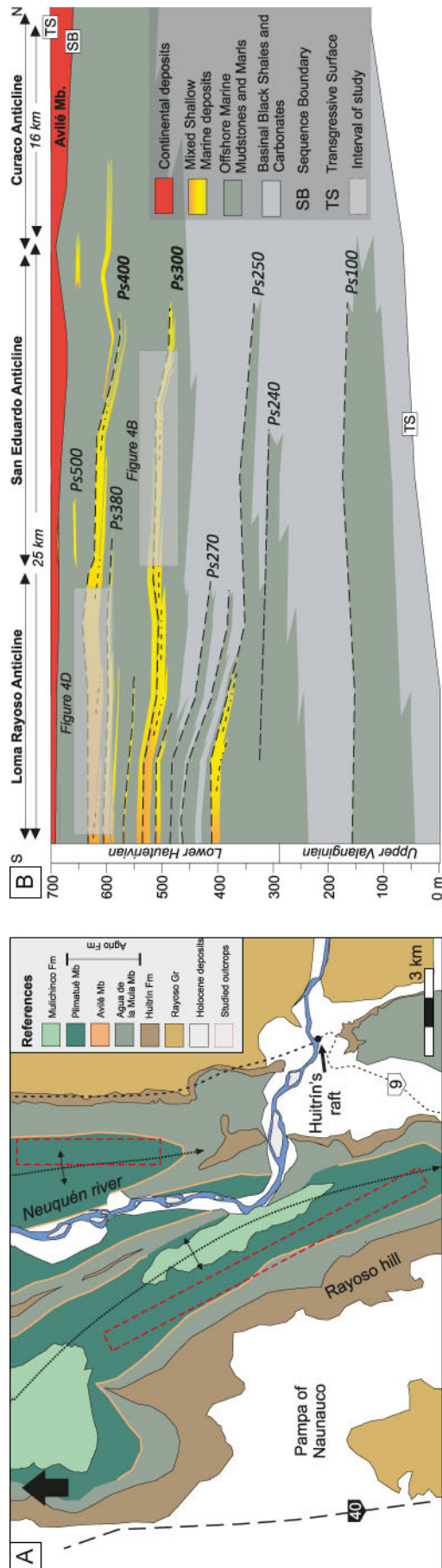
Figure 2. a) Location of the study area within the Neuquén Basin. b) Chronostratigraphic chart of the Mendoza Group (Kimmeridgian – Barremian).

early Hauterivian (Fig. 2b), under a climatic regime characterized by arid conditions (Scotese, 2000). Ubiquitous throughout the Neuquén Basin, this unit overlies the Mulichinco Formation composed of continental or shallow-marine deposits (Schwarz and Howell, 2005), and is abruptly truncated by fluvial and aeolian deposits of the Avilé Member

(Veiga *et al.*, 2007). The Pilmatué Member comprises up to 650 m thick of dark shales and marls that reflect offshore/basinal conditions and subordinated sandstones, representing shallow-marine accumulation in a wave-dominated shoreface system (Lazo, 2005; Spalletti *et al.*, 2011; Schwarz *et al.*, 2018). The system was compositionally defined as siliciclastic-dominated whereas carbonate deposits may form pure packages or mixed successions combined with terrigenous sediments (Schwarz *et al.*, 2018). However, towards the north of the basin the carbonate content of the deposits becomes more important even reaching to configure a carbonate ramp (Sagasti, 2005). Due to the development of regional-scale structural belts such as the Agrio fold-and-thrust belt, the Cretaceous stratigraphy (including the Pilmatué Member) of the basin have great exposures (Fig. 3a).

Mixed (carbonate-siliciclastic) shallow-marine deposits dominate the succession of the Pilmatué Member in the Agrio Fold and Thrust Belt. These deposits have been interpreted as the deposition under a wave- and- storm-dominated offshore-shoreface depositional system (Isla *et al.*, 2018; Schwarz *et al.*, 2018). Five main facies associations were defined within the preserved stratigraphic record (Table 2) whose vertical/lateral arrangement defines a typical shallowing-upward succession. Each succession is characterized by basal offshore bioturbated mudstones that are vertically replaced by siltstones interbedded with hummocky cross-stratified sandstones interpreted as offshore-transition deposits. These deposits grade into very fine-grained sandstones with ripple lamination, hummocky or swaley cross-stratification accumulated in a lower-shoreface setting. At the top of each parasequence, upper-shoreface and foreshore deposits are recorded and are the focus of the present contribution. Capping the shallowing-upward successions, a sixth facies association consisting in shell beds was interpreted as wave-ravinement deposits (Isla *et al.*, 2018). Reworking of previously accumulated shoreface deposits during minor transgressive episodes was responsible for the concentration of residual sediment such as large bioclasts, ooids and gravels, which formed the carbonate-dominated shell beds (Table 2).

Schwarz *et al.* (2018) defined these coarsening-upward cycles as parasequences and recognized up to 17 of them in the Pilmatué Member within the



study area (Fig 3b). These shallowing-upward units are limited by regional-scale flooding surfaces (Van Wagoner *et al.*, 1990). In general, parasequences or high-frequency sequences (according to Zecchin and Catuneanu, 2013), are 30 to 50 m thick and show good exposure of their internal architecture and excellent lateral continuity in a dip direction, which allowed to perform a high-resolution sedimentary analysis at intra-parasequence scale (Fig. 3b). The identification and correlation of vertical and lateral changes of facies associations allowed defining several bedsets and bounding surfaces within each parasequence. The lateral continuity of outcrops allowed tracking bounding surfaces and internal surfaces with confidence. The criterion used to define these minor cycles as bedsets is related to the relative deepening degree of the transgressive bounding surface, and hence the associated magnitude of shoreline shift (Isla *et al.*, 2018). The deepening degree associated to bedset boundaries corresponds to a vertical change of one or two facies belt (e.g. offshore transition deposits on top of lower shoreface or upper shoreface deposits), which would represent a shoreline displacement up to 5 km (Schwarz *et al.*, 2018). This magnitude of shoreline displacement is significantly minor than those related to parasequence boundaries of the Pilmatué Member, which had been estimated in the order of 20 km (Schwarz *et al.*, 2018). Nevertheless, bedset boundaries are not exclusively related to shoreline shift and their recognition may be limited to relative short distances along depositional dip and strike (Zecchin *et al.*, 2017).

DATASET AND METHODS

The dataset used here consists of two large (12 and 16 km) outcrop transects that trend WNW-ESE (Fig. 3a) and correspond to the strata of two individual parasequences: PS300 and PS400 (Fig. 3b). The full extent of these parasequences has been mapped

Figure 3. a) Location map of the study areas. b) The Pilmatué Member presents shallow-marine units, defined as parasequences, prograding to the north, that grade from shallow deposits to offshore and then to basin deposits (modified from Schwarz *et al.*, 2018). White rectangle marks the studied interval corresponding to the parasequences PS300 and PS400.

Facies associations	Lithology	Thickness	Sedimentary structures	Traces; Ichnofacies	Fossils	Interpretation
Offshore (O)	Mudstones grading to siltstones. Scarce very fine sandstones beds	2-10 m	Horizontal lamination or massive	Scarce <i>Palaeophycus</i> and <i>Teichichnus</i> . IB: 4-5 and 2-3. <i>Cruziana</i> ichnofacies	Ammonites. Molds of <i>Cucullaea</i> sp. and <i>Trigonia</i> sp.	Very low-energy conditions and settling processes. Across-shelf flows changed of sediment. Bathymetrically below the SWB
Offshore transition (OT)	Intercalated mudstones and siltstones with sand discrete beds. Subordinated very fine muddy sandstones	0,2-3 m	Massive mudstones and siltstones. Sandstones with HCS or ripple-cross lamination. Also massive muddy sandstones	Mainly <i>Palaeophycus</i> , <i>Planolites</i> , <i>Cylindrichnus</i> , <i>Ophiomorpha</i> and <i>Teichichnus</i> . IB: 2-4 and 5-6. <i>Cruziana</i> ichnofacies	Very few molds of <i>Cucullaea</i> sp.	Settling from suspension during fair-weather conditions alternating with oscillatory and combined flows during storm conditions. Bathymetrically between SWB and FWB
Lower Shoreface (LS)	Very fine to fine-grained sandstones	0,5-8 m	Amalgamated HCS beds. Ripple-cross lamination and symmetrical to slightly asymmetrical ripples	Traces of <i>Palaeophycus</i> , <i>Planolites</i> , <i>Cylindrichnus</i> , <i>Gyrochortes</i> , <i>Ophiomorpha</i> and <i>Teichichnus</i> . IB: 1-2 and 4-5. Distal <i>Skolithos</i> ichnofacies	Very few molds of <i>Cucullaea</i> sp.	Oscillatory-dominated combined flows generated by waves. Bathymetrically between FWB and SZ
Shell beds (SB)	Pebbly mixed sandstones	0,1-0,3 m	Trough cross-lamination. Asymmetrical ripples/dunes	Absent	Scarce specimens of <i>Ceratostreon</i> sp, <i>Cucullaea</i> sp. and <i>Trigonia</i> sp.	Basal erosion and rework by wave-ravinement during transgression. Unidirectional flows vertically pass to oscillatory-dominated combined flows

Table 2. Facies associations chart.

and reported in detail in previous studies (Schwarz *et al.*, 2018 for the PS300 and Isla *et al.*, 2018 for PS400). The selected transect of each parasequence for the present study consists of near-continuous exposures, which allowed describing the shoreface and foreshore strata (facies and architectural elements) in great detail.

The parasequence PS300 was studied in the San Eduardo anticline, located near the town of Chos Malal, in northern Neuquén province (Argentina) (Figs. 3a, 4a). It was mapped for over 18 km along depositional dip, showing a northward gradual thickening from 20 to 50 m. The parasequence PS300 represents the progradation of the shoreline for at least 16 km in a roughly northward direction (Schwarz *et al.*, 2018). The reconstructed shoreline trajectory using the boundary between upper-shoreface and lower-shoreface facies belts (Hampson, 2000), suggests a regressive trajectory with minimum

aggradation. Internally the parasequence PS300 has been subdivided in 5 bedsets (BS300.1 to BS300.5; Fig. 4b), comprising small scale (<10 m thick) coarsening-upward successions. Bedsets are defined as concordant successions of genetically related beds within parasequences, limited by surfaces of no deposition or erosion, and their correlative conformities (Van Wagoner *et al.*, 1990). A 600-m long outcrop where two-dimensional exposure of the PS300 deposits runs north-south was used for the architectural analysis (Fig. 4a). Fifteen sedimentary sections (1:10 scaled), were logged every 40 m and 2D sketches were drawn in the field. Dip and dip-direction of bed boundaries, and paleocurrents (total of measurements: 98) from trough cross-bedding and ripple crests were measured.

The parasequence PS400 was studied in the Loma Rayoso anticline located in the southern margin of the Neuquén River (Figs. 3a, 4c). The

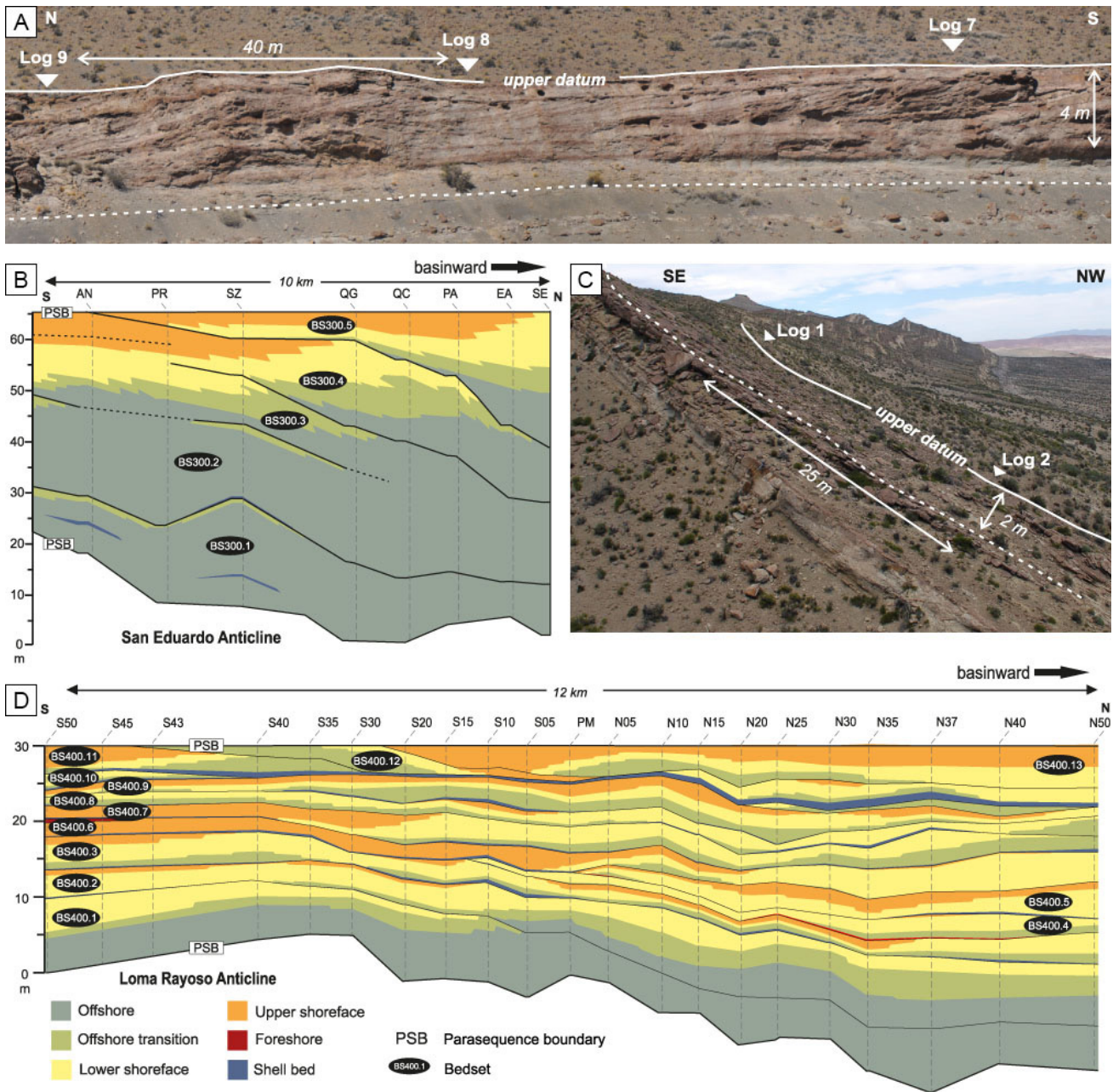


Figure 4. a) Outcrop view of the San Eduardo anticline where the deposits of the parasequence PS300 are better exposed. b) Correlation panel of the parasequence PS300 showing the five identified bedsets. c) Outcrop view of the Loma Rayoso anticline. d) The parasequence PS400 exhibit thirteen bedsets bounded by shell beds deposits. Dash lines: 1:50 logged sections within each parasequence; Arrows: 1:10 logged sections within nearshore deposits.

area is 12 by 5 km, and is part of the southwest flank of the anticline whose axial trace is oriented approximately N30°W. This parasequence is 30 to 40 m thick and it was mapped in detail for 12 km. Because the area is located in a more proximal section of the parasequence than in the previous unit (Fig. 3b), upper shoreface and foreshore deposits are relatively more abundant. Thirteen bedsets

(BS400.1 to BS400.13; Fig. 4d) were defined within the parasequence PS400 (Isla *et al.*, 2018). Most of the identified bedsets were recognized across the whole study area, but some of them are missing in the southern sector due to truncation (Fig. 4d).

During field work, 28 sedimentary logs at a scale of 1:50 were measured along, spaced ~500 m, for over 12 km (Fig. 4c). Also, 40 sedimentary

logs at a scale of 1:10 were incorporated following a space between them of 15 to 40 m, for over 1 km. Paleocurrent data (total of measurements: 98) was obtained mostly from trough cross-stratified facies and large-scale inclined beds. The compilation of all outcrop information, added to thin section observations, led to carry out a facies analysis. Sedimentary facies were grouped in facies associations considering interpretation of depositional processes and hydrodynamic regimes within the depositional system.

The architectural analysis of upper-shoreface and foreshore deposits was based on the classical concepts and methods of architectural-element analysis (Miall, 1985, 1988). The nature of bounding surfaces (erosional or concordant), and their scale and geometry were described. This approach allowed identification of the extent and geometry of different rock bodies as well as the distribution of facies within them. These depositional units were nested in terms of their scale and the intervening sedimentary processes to establish different hierarchies. This work allowed identifying different architectural styles in both parasequences. Each architectural style is composed of a specific set of orders of bounding surfaces, representing different hierarchies of discontinuities. Four hierarchies were defined and numbered for each architectural style.

Vertical and lateral changes of facies associations allowed the identification and correlation of several bedsets and their bounding surfaces. Also the variability of different sedimentary attributes (number of units, thickness, and proportions of carbonate-siliciclastic grains) among successive bedsets was analyzed to compare the deposits of identified shoreline morphologies. Detailed logs were measured exclusively focusing on the upper-shoreface and foreshore facies associations (Figs. 4b and c). This high-resolution outcrop dataset involving grain-size distribution, carbonate-siliciclastic grains, paleocurrents was combined with 2D sketches and high-resolution photomosaic to enable analysis of the two-dimensional distribution of the preserved deposits. New elements as beds geometries, orientation and hierarchy of heterogeneities were incorporated to the previous facies analysis. The photomontages comprise a set of photos with 30% mutual overlap that allowed bed tracing and measurement. Paleocurrent data were obtained mostly from trough cross-stratified facies

and seaward-dipping, inclined beds. These data were structurally restored and statistically analysed using the GEOrient Software, and presented as rose diagrams in order to establish sediment transport directions. Thin sections of representative facies were studied, focusing on grain-size distribution and contribution of siliciclastic versus carbonate grains.

ARCHITECTURAL STYLE 1

Facies distribution and depositional architecture

The most frequent architectural style (AE1) recognized in both parasequences is characterized by meter-scale, trough cross-bedded sandstones within the upper shoreface (Fig. 5a), and planar lamination in the foreshore deposits (Fig. 5b). Specific attributes of this architectural style have been already documented in a previous contribution (Isla, 2019).

The upper-shoreface deposits are up to 2 m thick and consist in mixed (carbonate-siliciclastic), pebbly sandstones and/or pure siliciclastic, fine-grained sandstones. Shell fragments (from fine- to medium-grained gravel) and ooids (up to coarse-grained sand) dominate at the base of the cross-bedding sets. Siliciclastic pebbles are dispersed and consist mainly of quartz and igneous rock fragments. When fragmentation is fairly low, bivalves such as *Cucullaea sp.* and *Trigonia sp.* are identified. Sedimentary structures consist in trough or planar/tangential cross-stratification (Fig. 5a), forming beds up to 2 m thick. Thickness of cross-stratified sets varies from 0.2 to 1 m, with a mean of 0.3 m. Individual sets consist of concave up, erosive-based lenses that range between from 0.5 to 2 m wide. In some cases, laterally and vertically stacked sets may form 3-5 m wide co-sets, bounded by erosive concave-upward surfaces. Bioturbation intensity is low (BI 1-2) and is largely dominated by *Ophiomorpha*. The measured palaeocurrent data from these trough cross-bedded sandstones showed a consistent low-angle obliquity (0 - 30°) with respect to the reconstructed shoreline (Fig. 5c).

Overlying these cross-bedded facies, there are up to 2 m thick intervals consisting in fine-grained sandstones dominated by planar lamination (Fig. 5b). In some cases, soft-sediment deformation structures, with no evidence of vertical or lateral displacement, may also be present. Planar lamination form beds,

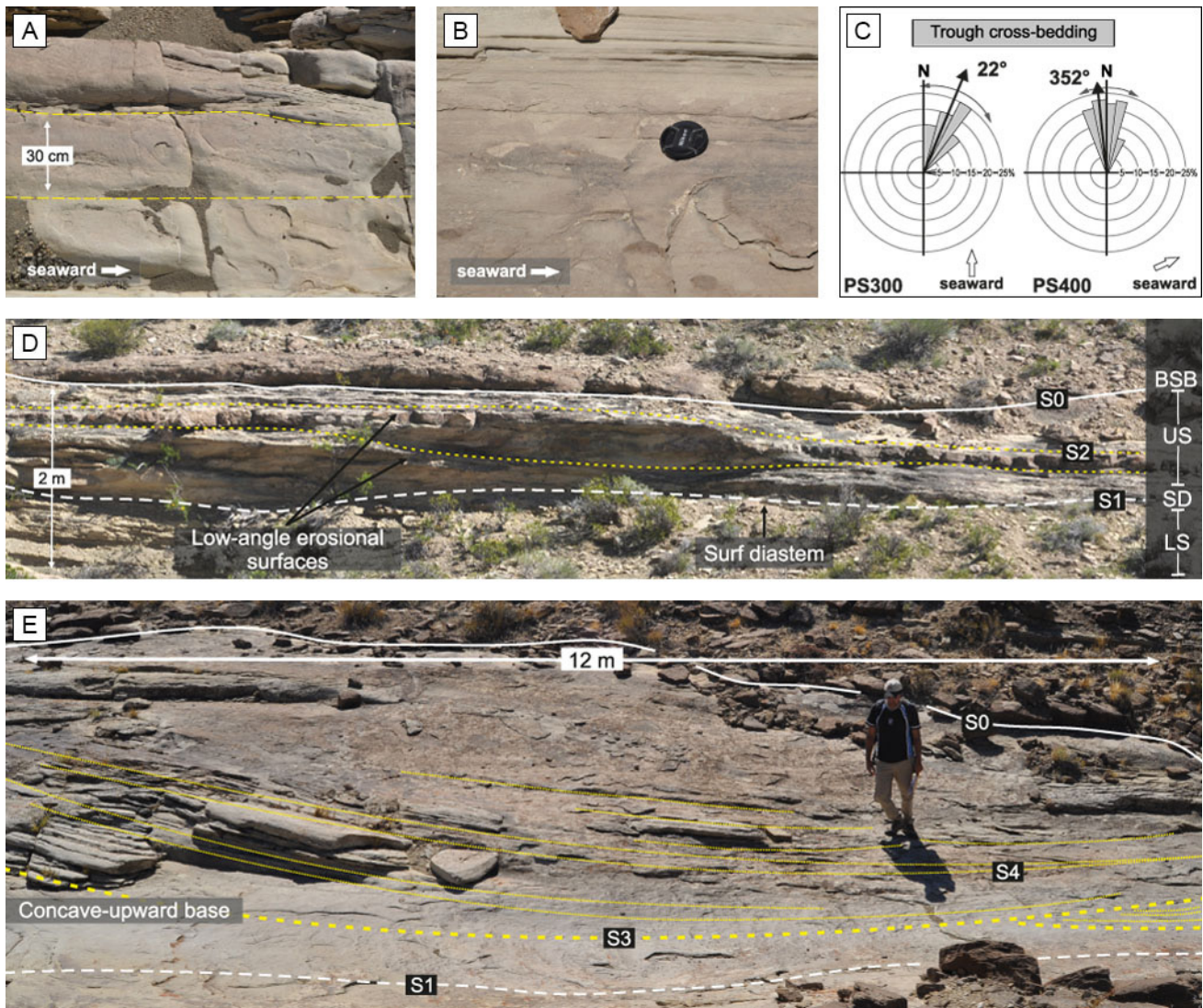


Figure 5. a) Outcrop view of typical upper-shoreface deposits, characterized by trough cross-stratification. b) Foreshore deposits usually show a thickening-upward trend in the planar lamination. c) Paleocurrent data measured from parasequences PS300 and PS400. d) Outcrop view of foreshore deposits commonly exhibit up to 12 m wide, concave-upward, symmetrical surfaces with planar lamination filling the scour. e) The contact between lower-shoreface (LS) and upper-shoreface (US) deposits is characterized by an erosional surface (S1) associated with a grain-size increase termed surf diastem (Zhang *et al.*, 1999; Swift *et al.*, 2003). Both upper-shoreface and foreshore (Fs) deposits are capped by transgressive surfaces defined as bedsets boundaries (BB). Also, low-angle erosional surfaces were identified within the upper-shoreface deposits.

within which lamination thickens-upward from 0.3 to 1 cm. This facies association is very conspicuous, dominating in the southern part of the outcrop (proximal section), where it always overlies upper-shoreface deposits. Bioturbation is completely absent; but wood fragments may be present.

Altogether, the upper-shoreface and foreshore deposits range in thickness from 0.5 to 3 m. Within these packages, the architectural analysis suggests the development of four hierarchies of bounding surfaces (S1^b to S4^b), based on their extension,

geometry, truncation relationships and facies contrasts across the surface. Transgressive surfaces associated with boundaries of genetic units as bedsets (S0) were excluded from the analysis. Surfaces include: 1) first-order surfaces (Fig. 5d) correspond to the boundaries of upper-shoreface and foreshore deposits (S1^b), 2) second-order low-angle surfaces (S2^b), bounding large-scale lenticular bodies within the upper-shoreface deposits (Fig. 5d), 3) third-order, concave-upward surfaces were identified in both upper-shoreface and foreshore deposits (Fig.

5e; S3^b), 4) fourth-order surfaces represented by the base of individual trough cross-bedding sets (S4^b).

Interpreted shoreline morphology

These deposits were interpreted as having accumulated in a clastic shoreline, more specifically displaying a bar-trough configuration (Fig. 6a, b). The presence of trough or planar cross-stratification suggests the formation and migration of sinuous crested dunes under a current-dominated, upper-shoreface setting (Greenwood and Mittler, 1985; Schwartz and Birkemeier, 2004; Clifton, 2006). These dunes would have formed within troughs or rip channels generated between large-scale bars (Fig. 6a), where unidirectional-dominated, combined flows were generated by the interaction between asymmetric oscillatory waves and strong longshore or rip currents (Wright *et al.*, 1991; Clifton, 2006). The lack of interpreted bar-related facies is due to their low potential of preservation within the fossil record (Davidson-Arnott and Greenwood, 1976; Hunter *et al.* 1979; Clifton, 2006; Isla, 2019). The constant obliquity of palaeocurrent directions inferred from trough cross-stratification relative to the orientation of the palaeoshoreline (Fig. 5c), suggests that dunes mostly migrated alongshore, under the influence of longshore transport processes (Fig. 6b).

Furthermore, the presence of planar lamination within the foreshore indicates upper-flow regime conditions, which take place within the intertidal section where swash and backwash processes associated with breaking waves occur (Masselink and Puleo, 2006). Also, the presence of soft-sediment deformation and the absence of bioturbation suggest that the foreshore was a high-energy, turbulent and stressful environment that inhibited organism colonization (MacEachern and Pemberton, 1992).

Concave-upward surfaces (S3^b) associated with the base of planar-laminated foreshore deposits (Fig. 5e), are interpreted as the sediment fill of semi-permanent intertidal channels. This type of intertidal morphology is typical of ridge-runnel configurations (Greenwood and Davidson-Arnott, 1979; Wijnberg and Kroon, 2002), where nearshore sand bars are welded to the beach during their onshore migration (Wright and Short, 1984). The currents within the runnels were possibly connected with the associated longshore channels (Aagaard *et al.*, 2006).

An additional criterion for interpreting a bar-

trough configuration of the shoreline is the presence of a well-defined erosional surface at the boundary between the upper shoreface and lower shoreface (S1^b). This surface termed surf diastem (Zhang *et al.*, 1997; Swift *et al.*, 2003; Clifton, 2006; Figs. 5c, 6a), marks an abrupt increase in grain-size between the very fine grained sandstones of the lower shoreface and the fine-grained or mixed pebbly sandstones of the upper shoreface (Fig. 5a). These erosional surfaces are commonly marked by the coarsest sediment available in the system (Hunter *et al.*, 1979; Clifton, 2006). Finally, the slightly erosional, low-angle surfaces defining large-scale lenticular sand bodies (S2^b; Fig. 6c) have been interpreted as the preservation of the shoreface profile related to the erosion of major storm events (Isla, 2019).

ARCHITECTURAL STYLE 2

Facies distribution and depositional architecture

This architectural style (AE2) is characterized by large-scale inclined beds and its facies distribution is closely related to the geometry of these beds (Fig. 7a). In contrast with the AE1 where there is a clear separation between upper-shoreface and foreshore deposits, the tangential beds show a systematic distribution of different facies from foresets to bottomsets. Planar lamination is ubiquitous in the foreset segments (Fig. 7b), both in fine-grained siliciclastic sandstones, and in fine- to lower medium-grained bioclastic sandstones. The textural attributes of mixed deposits is quite similar to those previously described for barred morphologies, i.e. shell fragments and ooids are up to fine- to coarse-grained sand. Concentrations of carbonate grains form bands that alternate with less concentrated bands, defining a lamination. Towards the bottomsets, small-scale trough and ripple cross-lamination becomes common (Figs. 7c and 7d), together with asymmetric ripples migrating onshore. Bioturbation varies from very low in the foresets to low in the bottomsets, and is represented by *Ophiomorpha* and subordinate *Teichichnus*. The inclined beds overlie and eventually, pass laterally to sub-horizontal beds mostly comprising lower-shoreface bioturbated sandstones (Fig. 7e; Isla *et al.*, 2020).

Three hierarchies of surfaces (S1^{nb} to S3^{nb}) were defined in the architectural analysis of these

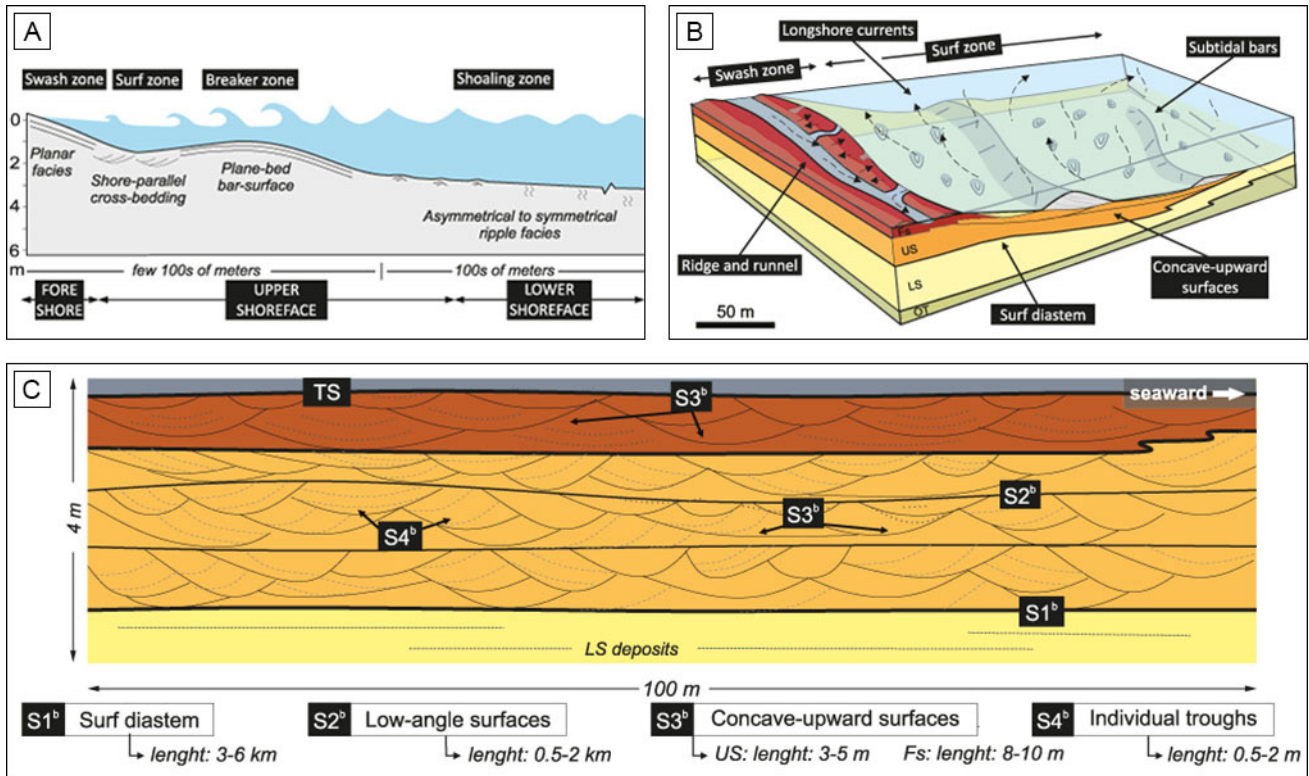


Figure 6. a) Cross-shore section for low- to moderate-gradient, barred clastic shorelines commonly associated with a wide surf zone and waves breaking far from the shoreline. Dunes in troughs and a plane bed in the swash zone preserved in the rock record as trough cross-bedded upper-shoreface deposits and planar-laminated foreshore deposits, respectively (modified from Clifton, 2006). b) Depositional model of a bar-trough shoreline showing the influence of longshore currents in the nearshore sediment transport. c) Preserved architecture of the barred shoreline deposits with different hierarchies of discontinuities. The surf diastem at the base is continuous for over few kilometers and marks an erosional contact with the underlying lower-shoreface deposits. Lenticular geometries, 0.5 to 2 km wide, are limited by low-angle surfaces. Minor discontinuities within these lenticular bodies, bound amalgamated sets of trough cross-bedded sandstones.

upper-shoreface/foreshore deposits. The boundary between the underlying lower-shoreface deposits and the upper shoreface/foreshore is not represented by a sharp surface, and is instead transitional. Foresets are commonly grouped in packages and such packages form sets that may show different dip orientations. These sets of foreset packages are bounded by erosional surfaces (S1^{nb}) that truncate the underlying packages (Fig. 7a). Truncation surfaces extend for over 300 to 1000 m (mean 600 m) and are associated with relatively abrupt changes in the dominant dip direction of foresets. Each set contain up to 6 packages of inclined beds oriented parallel to each other, but bounded by erosional surfaces with a scarp-like geometry (Fig. 7a; S2^{nb}). Finally, the foresets packages contain between 3 and 20 inclined beds limited by individual foresets (S3^{nb}). Beds immediately on top of these truncation surfaces are

enriched in coarse bioclasts and carbonate cement. The steep segment rapidly becomes sub-horizontal, but due the reddish distinct color of the associated deposits, these erosional surfaces can be traced down-dip into bioturbated sandstones. The downdip extension of erosional surfaces ranges from 30 to 150 m (mean 60 m) and they are spaced between them 20 to 40 m. Their dip direction is highly variable but always coincident with the quadrant towards which dipo of foresets are oriented.

The palaeocurrent data were measured mostly in the individual foresets (S3^{nb}) that dip dominantly from N to NW for the parasequence PS300 with a mean dip direction of N323.3°, while foresets measured within the parasequence PS400 dip from N to NE with a mean of 21°. In both cases, the average dipping direction of foresets is approximately shore-perpendicular.

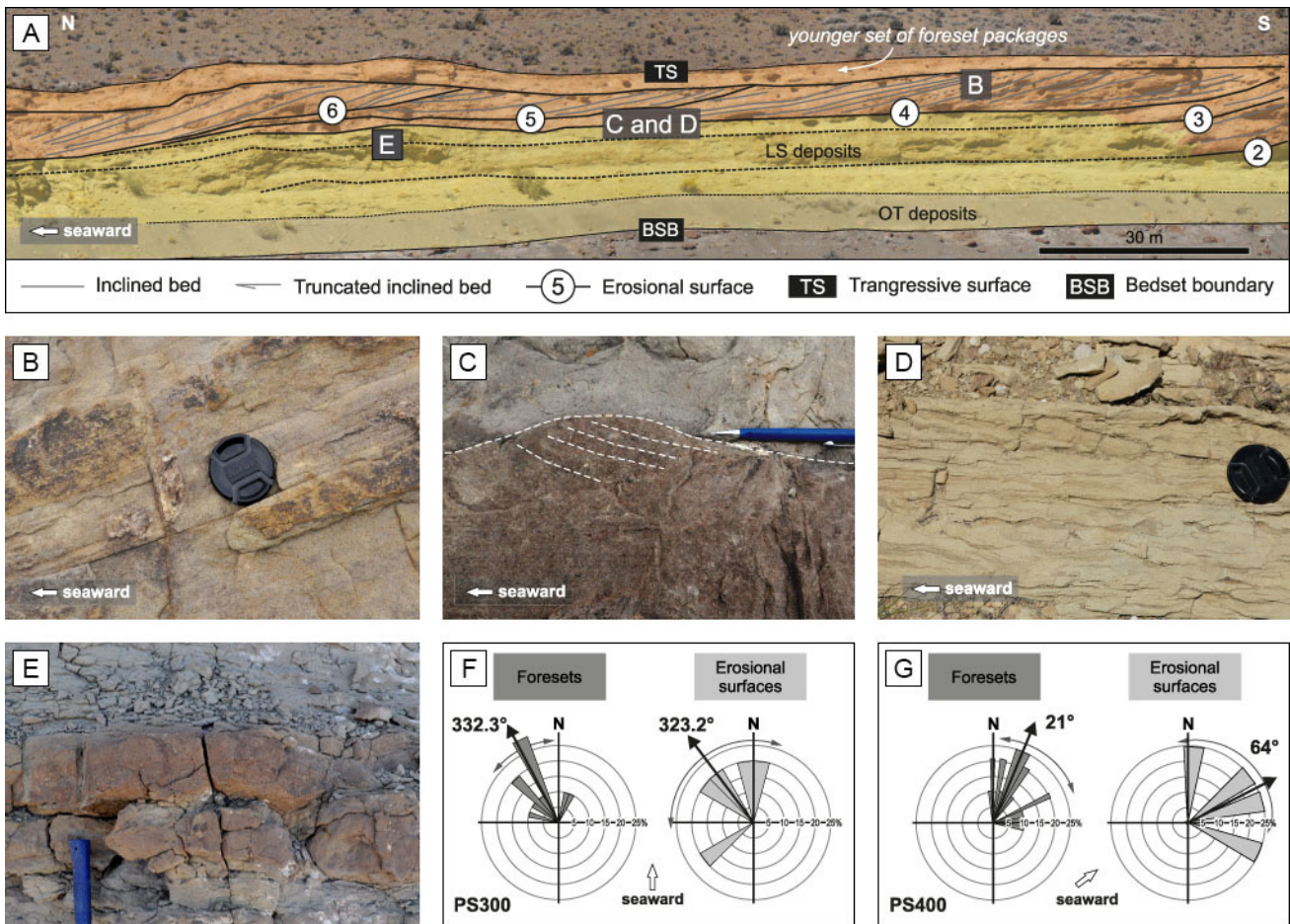


Figure 7. a) Interpreted photomosaic showing facies associations and detailed mapping of seaward-dipping, inclined beds. Most beds have tangential geometry (i.e., with foreset and bottomset segments) and can be traced for a few meters; but a few are bounded by more extensive surfaces that truncate underlying beds (here termed erosional surfaces and numbered from oldest (2) to youngest (6)). b) Foreset segment of inclined sandstone bed with internal planar lamination. c) Asymmetrical ripple in bottomset segment, dipping in an onshore direction. d) Very fine- to fine-grained sandstones with ripple lamination interpreted as lower-shoreface deposits. e) Highly bioturbated lower-shoreface sandstones. f) Paleocurrent data obtained within the parasequence PS300, from inclined beds and erosional surfaces. g) Paleocurrent data obtained within the parasequence PS400, from inclined beds and erosional surfaces.

Interpreted shoreline morphology

Much of the inclined beds are composed of planar-laminated facies, parallel to the beds related to swash and backwash processes (Fig. 8a; Reading and Collinson, 1996; Plint, 2010). Contrary to the Architectural Style 1, where upper shoreface was characterized by trough cross-stratification, these deposits lack of facies that could suggest the presence (and preservation) of dunes related to wave-generated currents. The widespread development of plane bed seems to be favored when the surf zone is narrow or even inexistent and the swash zone is wider than the surf zone (Aagaard *et al.*, 2013). The sedimentation associated with the surf

zone could be attributed to the small-scale trough cross-stratification characterizing the bottomsets of inclined beds.

The interpretation of a narrow, or even inexistent, surf zone as well as an extensive development of the swash zone would be directly linked to the steepness of the nearshore seabed profile, as the steeper profile, the narrower the surf zone. In this context, the large-scale inclined sandstone beds described have been interpreted to represent high-gradient, marine depositional profiles, of a non-barred configuration (Fig. 8b; Isla *et al.*, 2020). Most of this non-barred profile was covered by planar-laminated facies produced under oscillatory or combined flows (Schwartz and Birkemeier, 2004), and without a

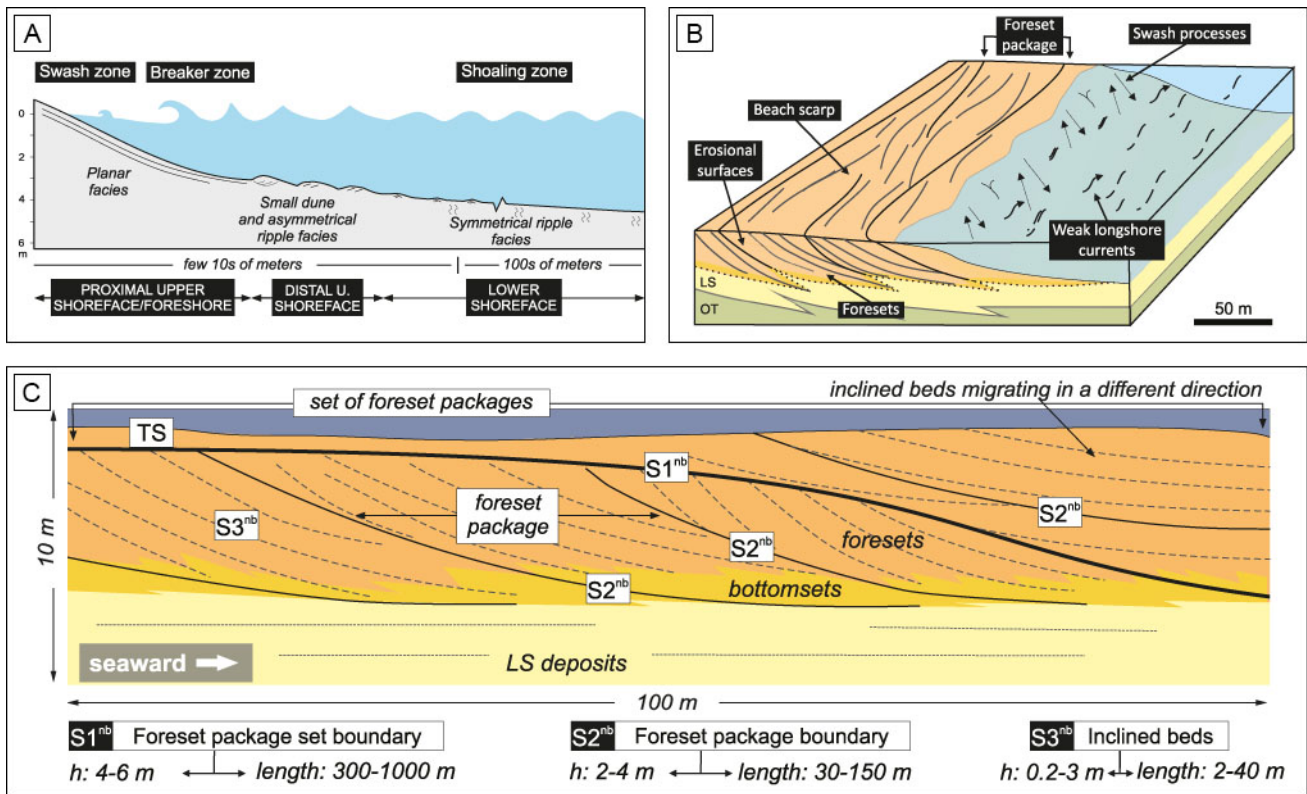


Figure 8. a) Cross-shore section reconstructed for a clastic shoreline where bars cannot develop. Planar-laminated sands would be persevered in the rock record as the dominant sedimentary facies both in the foreshore and in the proximal upper shoreface of these non-barred shoreline systems. b) Depositional model of a high-gradient, non-barred clastic shoreline characterized by a steep profile ($> 5^\circ$). Given the gradient, the surf zone must have been narrow or non-existent, while the swash zone become wider. c) Preserved architecture of the non-barred shoreline deposits with different hierarchies of discontinuities. Seaward-dipping inclined beds are grouped in foreset packages bounded by successive erosional surfaces. At the same time, foreset packages are grouped in sets of foreset packages showing different dipping directions.

distinct facies break between the foreshore and the proximal upper shoreface. Seaward of the breaker zone (i.e., in the distal upper shoreface), onshore-migrating asymmetric ripples and small dunes were commonly formed and preserved (Fig. 8b), most likely under oscillatory-dominant flows (Clifton, 2006; Cummings *et al.*, 2009). A non-barred setting is also supported by the absence of a surf diastem and the consistent seaward accretion of foresets and foreset packages for hundreds of meters with no landward dipping surfaces (Fig. 8c).

Successive seaward-dipping foresets ($S3^{nb}$) represent the accretion of upper-shoreface/foreshore deposits during shoreline progradation, regularly-spaced erosional surfaces recognized (Fig. 8c). At the same time, bounding foresets packages ($S2^{nb}$) are interpreted to represent beach scarps generated during stages of beach retreat (Fig. 8b). These surfaces represent significant sediment erosion and

export to the lower shoreface that can be triggered by exceptional storms or periods of high wave energy (Isla *et al.*, 2020). The presence of first-order surfaces bounding sets of foreset packages ($S1^{nb}$) and the abrupt changes in the dominant dip orientation would be related to beach rotation processes (Anthony, 2008; Davison-Arnott, 2010), associated with major-scale reconfigurations of the nearshore system, as seen in beach-ridges set boundaries (Otvos, 2000; Tamura, 2012).

INTRA-PARSEQUENCE ANATOMY

The detailed facies and architectural analysis of upper-shoreface and foreshore deposits allowed interpreting two different shoreline morphologies (Figs. 6b and 8b), recorded within the progradation of each parasequence (Fig. 9) and corresponding to a barred and non-barred nearshore configuration

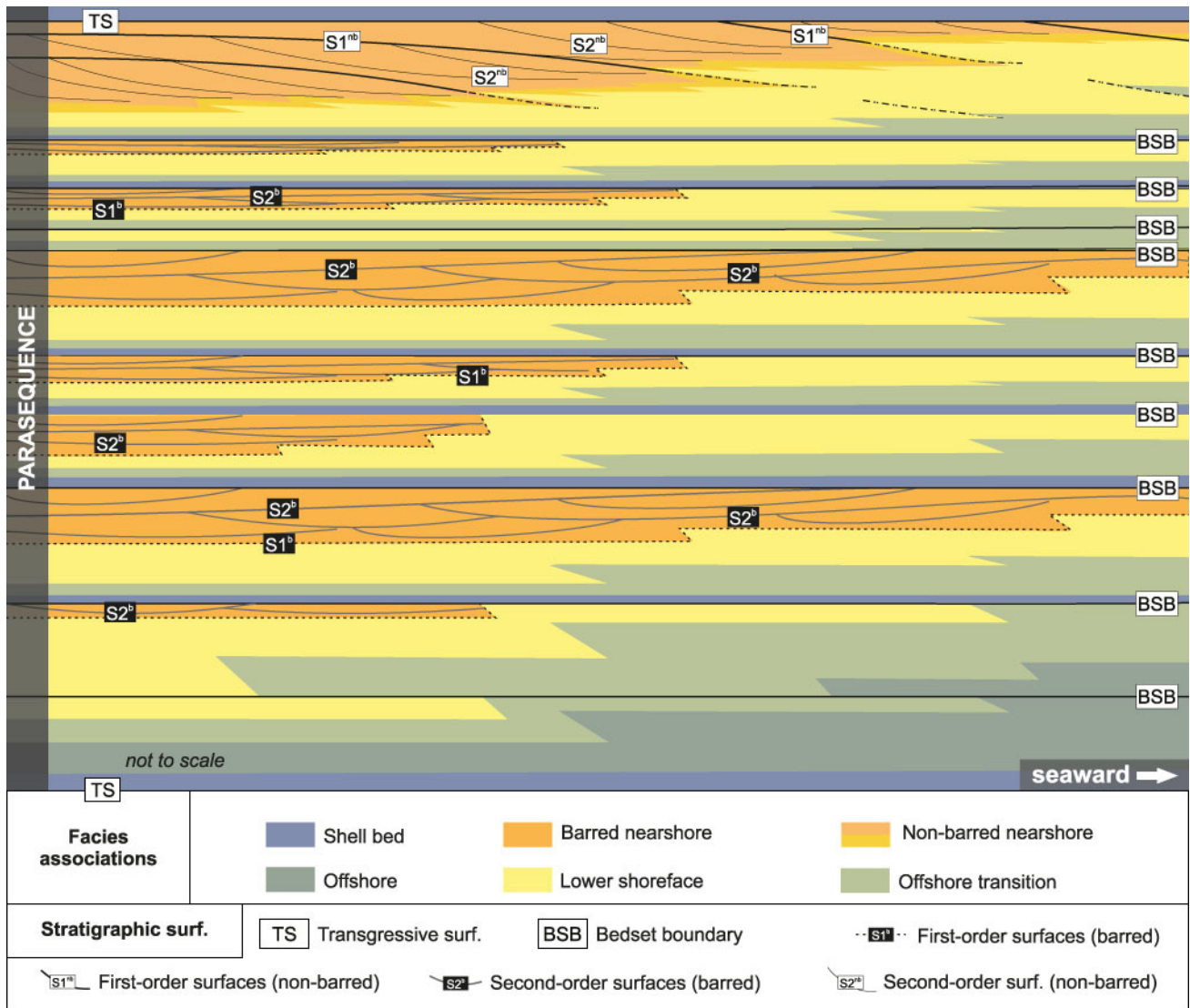


Figure 9. Summary of the reconstructed stratigraphic architecture (example from the parasequence PS400). Most bedsets were interpreted as the deposition within a barred clastic shoreline with exception of the uppermost of each parasequence, which have been interpreted as non-barred conditions.

that succeeded though time. Both the number of bedsets with upper-shoreface and foreshore deposits and their proportion in a parasequence indicate an important difference between barred and non-barred shoreline deposits. The first were recorded in the upper-shoreface and foreshore deposits of 10 bedsets (out of 13) of the parasequence PS400 and in 4 (out of 5) of the parasequence PS300, in both cases involving around the 90% of the total parasequence thickness (Table 3). On the contrary, non-barred deposits were exclusively recorded in the uppermost bedset of each parasequence, representing just 10% their cumulative of the thickness (Table 3). Thicknesses of upper-shoreface and foreshore deposits also mark an

important difference between the barred and non-barred record. In the first case, the average thickness is less than a meter (0.96 m), while for non-barred deposits they can reach 2.66 m (Table 3). When the thickness of lower shoreface is compared, values are quite similar (1.35 and 1.40 m). The shoreline trajectory for AE1 deposits commonly define an aggrading to low prograding evolution (high angle *sensu* Helland-Hansen and Martinsen, 1996), while for non-barred the shoreline trajectory has low angle corresponding to a moderate rate of progradation relative to aggradation.

The described transition from AE1 to AE2 architectural style is also correlated to changes in the

Shoreline type	Barred shoreline deposits	Non-barred shoreline deposits
N° of bedsets	PS300: 2 bedsets; PS400: 10 bedsets	PS300: 1 (BS300.5); PS400: 1 (BS400.13)
% of thickness (within the parasequence)	PS300: 83% (29.05 m); PS400: 90% (31.72 m)	PS300: 17% (5.95 m); PS400: 10% (3.28 m)
US + Fs average thickness (m)	0.96	2.66
LS average thickness (m)	1.35	1.40
Upper-shoreface facies	Trough cross-bedded sandstones and mixed sandstones	Foresets: dominant planar laminated sandstones and mixed sandstones; Bottomsets: trough cross-lamination sandstones and mixed sandstones
Foreshore facies	Planar laminated, fine-grained sandstones	
LS-US boundary	Surf diastem	Transitional
US-Fs boundary	Well-defined, concordant	Difusse, slope break
Mixed deposits (%)	67%	60%
Shoreline trajectory	Aggradating to low progradating	Moderate progradating

Table 3. Comparison of sedimentary attributes between barred and non-barred shoreline deposits.

proportion of carbonate and siliciclastic components (Table 3). The storm-dominated shoreface-offshore deposits interpreted for the Pilmatué Member are characterized by a limited abundance of carbonate grains such as bioclasts and ooids, which led to define it as a siliciclastic-dominated mixed system. However, the distribution of carbonate components is not homogeneous across the whole system but it is restricted to upper-shoreface and foreshore deposits. The abundance of carbonate particles within AE1 deposits (67%; Table 3) could be related to the effectiveness of longshore currents (Isla *et al.*, 2018; Schwarz *et al.*, 2018). However, AE2 deposits also have a high proportion of mixed deposits (60%; Table 3) suggesting that the influence of longshore currents was not the sole control. The abundance of carbonate grains within the proximal areas of the system was always constant during the evolution of the Pilmatué Member.

Changes in sediment transport dynamics for wave-dominated shorelines are intimately related to the wave behavior (Davidson-Arnott, 2010; Aagaard *et al.*, 2013). Barred coasts have been considered as the resulting morphology of dominantly dissipative conditions where the wave energy is more effectively

dissipated during their approach to the shore (Wright and Short, 1984). Dissipative coasts and nearshore bars are directly related to low gradients (Wijnberg and Kroon, 2002; Aagaard *et al.*, 2013; Hughes *et al.*, 2014), where sediment is continuously redistributed by longshore processes. On the contrary, non-barred coasts are closely related to more reflective conditions where weak longshore currents are not capable to redistribute sediment which tends to be accreted to the shore generating high-gradient and bar-less configurations (Isla *et al.*, 2020). The identified transformation in shoreline morphology, reflected in the rock record (Table 3), is the long-term response to a change in wave behavior from dissipative to reflective dynamics.

The larger thicknesses of upper-shoreface/foreshore deposits for non-barred conditions compared to barred conditions could be associated with a 'relative excess' of sediment budget within the proximal areas related to two aspects: the dominance of onshore sediment transport by swell waves typical of non-barred (reflective) conditions and the weakness of longshore currents that may redistribute the sediment alongstrike (Aagaard *et al.*, 2013).

RESPONSES TOWARDS DISTAL-SHOREFACE SETTINGS

Changes in shoreline morphology are associated with the nearshore setting, which represents the most variable and dynamic part of the marine depositional system (Davidson-Arnott, 2010). The distal parts of the shoreface should be also influenced by the long-term prevailing conditions of shoreline dynamics (i.e. waves, currents, sediment budget; Fig. 10a). The analysis of lower-shoreface facies correlatable to the described barred and non-barred deposits were analyzed. Each lower-shoreface interval was evaluated in terms of their proportions of facies generated by fair-weather and storm conditions, showing significant differences. The obtained results indicate that those bedsets where barred configurations were interpreted, present both types of facies in variable proportions (Fig. 10b). These lower-shoreface deposits are almost entirely composed of interbedded fair-weather ripple cross-laminated or highly bioturbated sandstones, with storm-related beds with hummocky or swaley cross-stratification (HCS and SCS) (Fig. 10c). Instead, intervals where non-barred shoreline settings were interpreted are exclusively composed of ripple-laminated and/or bioturbated sandstones deposited during fair-weather conditions (Fig. 10d). These lower-shoreface deposits completely lack of sandstones with HCS.

During extended fair-weather conditions, the dominant onshore transport and the dominant swell waves generate a net sediment transport to the proximal areas, “starving” the distal parts where no bars are constructed (Fig. 10a). These prevailing transport dynamics characterize non-barred morphologies, where there are important gradient differences between the nearshore and the lower shoreface. Instead, during storm conditions, the waves and down-welling currents transport masses of sediment seaward, which brings the necessary budget for bar building (Fig. 10a; Davidson-Arnott, 2010). Also, during storms the erosion of proximal areas and redistribution towards the outer part of the shoreface smooth the coast gradient.

The shoreface is an exchange and buffering zone dominated by friction, constantly changing in order to balance the sediment budget of the system (Fig. 10a; Swift, 1975; Niedoroda *et al.*, 1985; Cowell *et al.*, 1995; Anthony, 2008). Wave-climate changes impact

directly on the resulting shoreline morphology and they have a correlative expression towards the distal parts of the system, especially in those located above the depth of closure (Ortiz and Ashton, 2016). Even the sum of onshore-directed and offshore-directed flows for a coastal setting is balanced over short periods (Wright *et al.*, 1991); imbalances may occur among larger scales of time, due to the dominant cross-shore transport conditions. During fair-weather conditions, wave-dominated shorelines are dominantly affected by swell waves, which transport much of the carrying sediment onshore, and hence produce the starvation of distal parts of the shoreface and the absence of bars (Fig. 10a; Davidson-Arnott, 2010). On the other hand, storm-waves tend to export sediment towards the distal areas favoring the building of bars. In that sense, because of their distinct wave properties and transport dynamics, fair-weather and storm processes generate two different lower-shoreface architectural styles and facies successions. During fair-weather, the shoaling zone is mostly covered by symmetric to asymmetric ripples produced by oscillatory-dominated combined flows and an intense organic activity favored by the well-oxygenated water column (Fig. 10a). On the contrary, the strong and high-amplitude storm waves produce hummocky bedforms that result in the preservation of sandstones with HCS. Storm processes also constitute stressful conditions of the environment that inhibit the colonization (Fig. 10a), limiting the benthic activity to escape traces of opportunistic fauna. There is a clear correlation between the morphology of proximal nearshore settings and the prevailing processes of sediment exportation, which are reflected in the preserved deposits of the lower shoreface.

Discussion: controls in the transition from barred to non-barred morphology

During the last two decades, several studies have analyzed the intra-parasequence stratigraphic architecture of deltaic and strandplain successions (Gani and Bhattacharya, 2007; Hampson *et al.*, 2008; Sømme *et al.*, 2008; Charvin *et al.*, 2010; Forzoni *et al.*, 2015). It is well known that high-frequency changes in depositional conditions triggered by autogenic or allogenic factors may occur resulting in the development of bedsets (Van Wagoner *et al.*, 1990). However, the high-resolution analysis of such

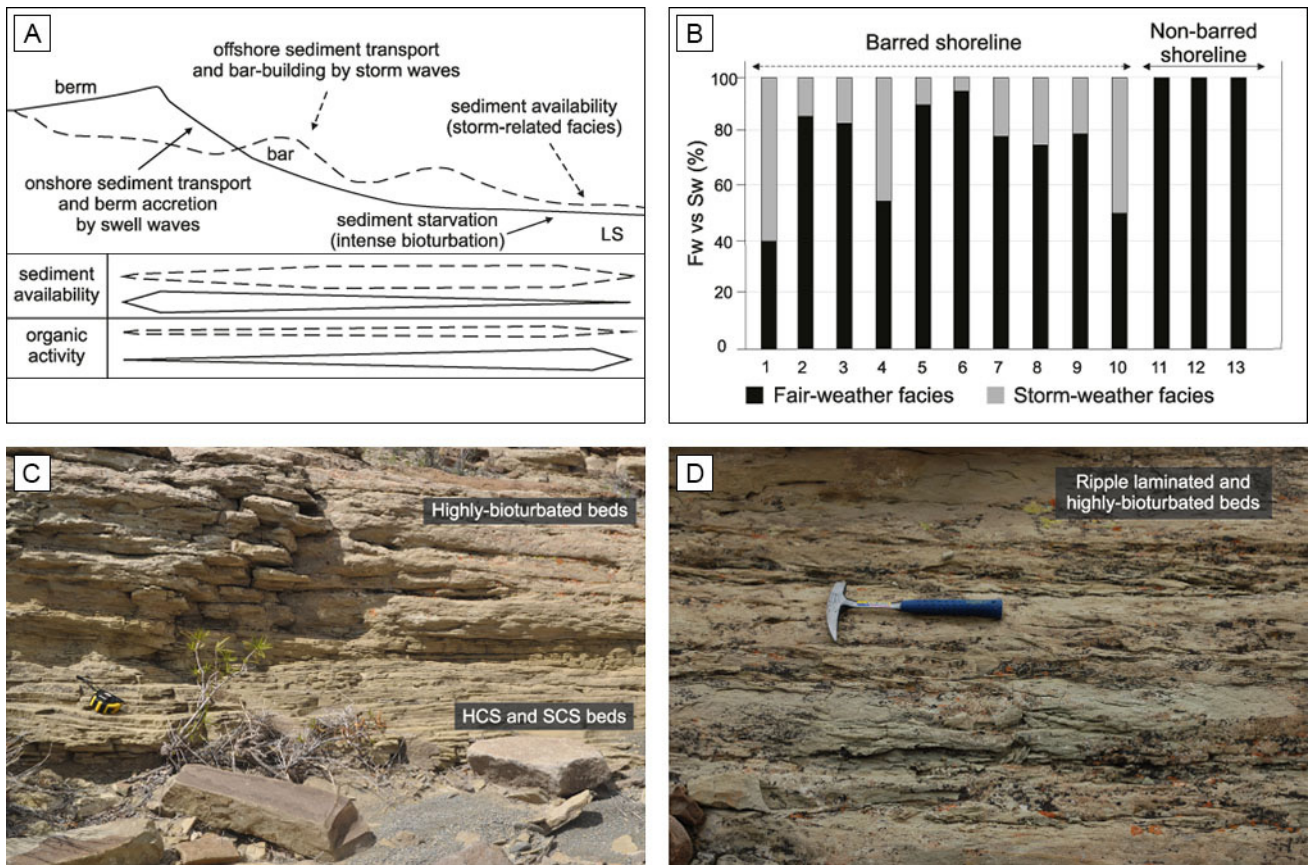


Figure 10. **a)** During storms, offshore-directed currents export sediment to the outer shoreface, where it eventually accumulates as building of nearshore bars. Instead, during fair-weather conditions, dominant swell waves transport sediment onshore, reducing the sediment budget in distal areas (modified from Davidson-Arnott, 2010). **b)** Proportions of fair-weather and storm facies within the lower-shoreface deposits of successive bedsets in the parasequence PS400 (black columns represent fair-weather facies and grey columns are storm facies). **c)** “Barred intervals” consist in the inter-bedding of storm-related (sandstones with HCS) and fair-weather facies (highly bioturbated sandstones). **d)** “Non-barred intervals” are exclusively composed of fair-weather facies (ripple laminated and highly bioturbated sandstones).

progradational wave-dominated successions has not documented significant changes in depositional facies and architectural elements as the ones described for the Pilmatué Member. The complex stratigraphic architecture reconstructed for the Pilmatué Member demonstrates other changes than the ones resulting from the development of bedsets and that result in different shoreline morphologies (Isla *et al.*, 2018). Such complexity combines with changes in sediment transport dynamics operating for longer, that result in different preserved shoreline morphologies (Figs. 6b and 8b). However, the defined three different scales of changes need to be framed in a sequence-stratigraphic context. The main processes associated with both ends of defined scales and hence, with development of parasequences and bedsets have been already discussed previously (Schwarz *et al.*,

2018; Isla *et al.*, 2018). The change in architectural style between bedsets and within a parasequence records an intermediate high-frequency change that occurred during the progradation of a single parasequence, but of a larger scale than the one responsible for the development of successive bedsets. The transformation of the shoreline morphology due to changes in depositional conditions could be explained by determinate controlling factor or even a combination of different factors therefore, operating at different scales (Heller *et al.*, 1993; Burgess *et al.*, 2006).

High-gradient profiles, where bar generation is commonly inhibited, are characteristic of reflective conditions, whereas for low-gradient profiles, the energy of waves is dissipated and used for building nearshore bars (Davidson-Arnott, 2010; Aagaard *et*

al., 2013). As a significant change in sediment grain-size -that may help explain the gradient change and therefore the transition to reflective conditions- has not been registered within the studied successions, this change must reflect the morphological responses to balance modifications in cross-shore and along-shore sediment budget. In that sense, an increase in the nearshore gradient could be related to a relative excess of sediment on the proximal parts of the shoreline system and different processes are proposed to explain the relative excess of sediment and consequent steepening of the nearshore, which result in the change from barred to non-barred conditions during the parasequence evolution.

The first possibility is that changes in the sediment budget of nearshore settings were associated with changes in the prevailing cross-shore and long-shore transport mechanisms (Fig. 11a). Low-gradient, sand-rich beaches are typically dissipative with a wide surf zone and an irregular cross-shore profile with nearshore bars and troughs. In this context, the influence of storms and longshore currents plays a key role in terms of sediment redistribution. Instead, high-gradient, sand-rich beaches tend to develop under reflective conditions where dominant swell waves result in an onshore sediment transport (Davidson-Arnott, 2010; Aagaard *et al.*, 2013). In this regard, the change from low gradient (barred) to high-gradient (non-barred), could be related to climatic oscillations, more specifically to wave-climate variations. Wave climate may be relatively constant for timescales of 10^2 to 10^3 years (Li *et al.*, 2015), but not necessarily for longer periods. Previous studies have demonstrated that wave-climate variations could generate imbalances in sediment budget at the scale of individual bedsets (Storms and Hampson, 2005; Isla *et al.*, 2018).

A second possibility is that the steepening of the nearshore could be related to long-lived prograding conditions, which eventually should result in large amounts of available sediment over the proximal settings. The studied parasequences of the Pilmatú Member constitute dominantly aggrading to prograding stratigraphic units that need a constant increase in accommodation to build-up. In that sense, the maximum rates of progradation should be reached towards the upper part of the parasequence, if accommodation increases relatively constant and the rate of sediment supply do not change. If the rate of relative sea-level rise remains constant, a higher

rate of sediment supply is necessary to balance the increasing accommodation and maintain the progradation. Therefore, the preferential occurrence of non-barred conditions towards the uppermost bedset within a parasequence (Fig. 9) could be associated with a long-lived high rate of sediment supply to the shore (Fig. 11b). These could be associated with large amounts of sediment that are accreted to the coast by onshore transport. If the mechanisms of exportation or along-strike redistribution are not efficient enough, the relative excess of available sediment within the proximal settings would result in the steepening of the nearshore, regarding the rest of the depositional profile. This increase of the nearshore gradient would trigger the formation of a prograding, high-gradient non-barred shoreline. Therefore, this model proposes the presence of high-gradient, non-barred conditions as a morphological response of the depositional profile due to long-lived normal regressive conditions.

Finally, the generation of non-barred conditions could also represent the prelude of depositional changes triggered during the deepening of the system, which eventually would result in the generation of a large-scale flooding surface (parasequence boundary). Under a protracted and slow relative sea level rise, without significant changes in sediment supply, the sediment budget may exceed the accommodation within proximal areas, but simultaneously be relatively smaller for the distal settings (Fig. 11c). Besides, the relative deepening generates the weakening of longshore currents, which are responsible of the sediment redistribution the system. If longshore transport, operating over the nearshore, is not efficient enough, it could trigger a sediment excess in the proximal area and a relative “sediment starvation” towards the outer parts of the shoreface-offshore system. If this situation remains, the adjustment of the system profile may result in a relative “autosteepening” or a passive increase in the gradient of the nearshore.

The proposed models explain a morphological response of the shoreline to ongoing changes on the prevailing transport conditions and particularly, to a relative increase in the available sediment over the nearshore settings. However, these changes in depositional conditions could be triggered by allogenic processes controlling the parasequence evolution, as relative changes in sea level or

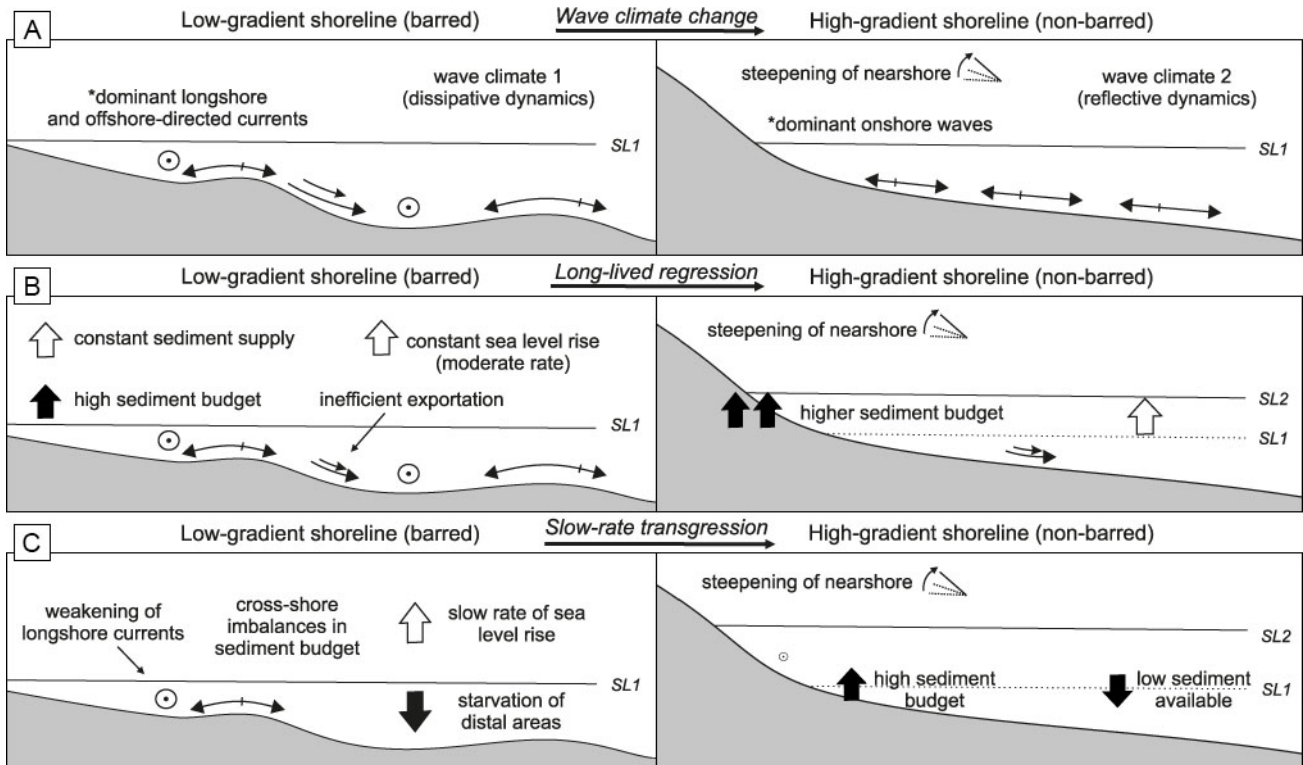


Figure 11. Possible models can be used to explain the transition from prevailing dissipative to reflective wave behavior, and hence from barred to non-barred conditions. **a)** Wave climate changes from dissipative to reflective conditions could be a feasible explanation for the steepening of the nearshore. In the first case, longshore and offshore-directed currents redistribute sediment within the depositional system; while in the latter, dominant swell waves generate high rates of onshore sediment transport. **b)** Under long-lived regressive conditions with constant sediment supply and sea level rise, if exportation mechanisms are not enough efficient, there is a relative “maximum sediment budget” in the proximal areas, resulting in a steepening of the nearshore. **c)** During transgressions, longshore currents tend to become less efficient due to the deepening of the water column, which result in a cross-shore imbalance of the sediment budget and a consequent starvation of distal parts.

changes in sediment supply. The vertical stacking of successive bedsets in both studied parasequences show a progradational stacking pattern with seaward migration of the shoreline up to the top (Figs. 4b and 4d), which seems to exonerate the possibility that non-barred morphologies were generated during transgressive conditions. Hence, the steepening of the nearshore and the consequent installation of non-barred conditions would be related to wave climate changes and/or long-lived regressive conditions.

CONCLUSIONS

The present work documents changes in shoreline morphology interpreted from the preserved depositional architecture of each studied parasequence (10^4 to 10^5 y). The facies and architecture of barred and non-barred deposits represent the dominant processes that governed the

hydrodynamic conditions of sedimentation, which prevailed over long-lived periods. The detailed analysis of the sedimentary facies and the depositional/erosional surfaces within the upper-shoreface and foreshore deposits of successive bedsets composing a parasequence led to reconstruct how the shoreline morphology may have changed from persistent bar-trough configurations to the absence of nearshore bars through time. Those changes also represent the transformation from a relatively low-gradient beach profile to a high-gradient profile due to the adjustment to new conditions in sediment transport dynamics. The transition from barred to non-barred conditions implicates that the coastal sediment transport shifted from a longshore-dominated to an onshore-dominated dynamics due to a weakening of wave-induced currents and strengthen of swell conditions.

There is an increasing requirement to incorporate

the analysis of upper-shoreface and foreshore deposits to the high-resolution depositional models of shallow-marine environments. Sequence stratigraphy either as a conceptual model or a methodology for understanding the sedimentary record is in constant metamorphosis of its concepts. Results led to propose a number of possible controls that could triggered the change from barred to non-barred conditions. Invariably, the proposed models are related to a mechanism of steepening of the nearshore profile due to a relative excess in the sediment budget compared to the rest of the system. The triggering mechanism for the steepening of nearshore settings may be related to climatic external changes (variations in wave climate), or to changes in the sequence-stratigraphic context (regressive or transgressive conditions). Based on the progradational stacking pattern of both studied parasequences, the transgressive model could be dismissed. Notwithstanding, more research in needed to be able to establish the dominant control. The interpretations made, suggest that mid-term evolution of clastic shorelines may result in a complex sequence-stratigraphic architecture. A better understanding of high-frequency processes operating and responsible from intra-parasequence changes is increasingly necessary.

Acknowledgments

Authors would like to thank CONICET, Universidad Nacional de La Plata and YPF S.A. for the financial support of this project. Also, authors would like to thank the Editor Sebastián Richiano as well as, Luca Colombera and Massimo Zecchin for their constructive reviews.

REFERENCES

- Aagaard, T., M. Hughes, R. Møller-Sørensen and S. Andersen, 2006. Hydrodynamics and sediment fluxes across an onshore migrating intertidal bar. *Journal of Coastal Research* 22: 247-259.
- Aagaard, T., B. Greenwood and M., Hughes, 2013. Sediment transport on dissipative, intermediate and reflective beaches. *Earth-Science Reviews* 124: 32-50.
- Ainsworth, R., S. Flint and J. Howell, 2008. Predicting coastal depositional style: influence of basin morphology and accommodation to sediment supply ratio within a sequence stratigraphic framework. In Hampson, G.J., Steel, R.J., Burgess, P.M., and Dalrymple, R.W., (Eds.) *Recent Advances in Models of Siliciclastic Shallow-Marine Stratigraphy*. SEPM, Special Publication 90: 237-263.
- Amorosi, A., L. Bruno, B. Campo, A. Morelli, V. Rossi, D. Scarponi, W. Hong, K.M. Bohacs and T.M. Drexler, 2017. Global sea-level control on local parasequence architecture from the Holocene record of the Po Plain, Italy. *Marine and Petroleum Geology* 87: 99-111.
- Anthony, E.J., 2008. *Shore processes and their palaeoenvironmental applications (Vol. 4)*. Elsevier, 518 pp.
- Berton, F., C.C.F. Guedes, F.F. Vesely, M.C. Souza, R.J. Angulo, M.L.C.C. Rosa and E.G. Barboza, 2019. Quaternary coastal plains as reservoir analogs: Wave-dominated sand-body heterogeneity from outcrop and ground-penetrating radar, central Santos Basin, southeast Brazil. *Sedimentary Geology* 379: 97-113.
- Bruno, L., K.M. Bohacs, B. Campo, T.M. Drexler, V. Rossi, I. Sarmartino, D. Scarponi, W. Hong and A. Amorosi, 2017. Early Holocene transgressive palaeogeography in the Po coastal plain (northern Italy). *Sedimentology* 64: 1792-1816.
- Burgess, P.M., H. Lammers, C. Van Oosterhout and D. Granjeon, 2006. Multivariate sequence stratigraphy: Tackling complexity and uncertainty with stratigraphic forward modeling, multiple scenarios, and conditional frequency maps. *AAPG Bulletin* 90: 1883-1901.
- Burgess, P.M., P.A. Allen and R.J. Steel, 2016. Introduction to the future of sequence stratigraphy: evolution or revolution?. *Journal of Geological Society* 173: 801-802.
- Catuneanu, O., 2019. Model-independent sequence stratigraphy. *Earth-Science Reviews* 188: 312-388.
- Charvin, K., G.J. Hampson, K.L. Gallagher and R. Labourdette, 2010. Intra-parasequence architecture of an interpreted asymmetrical wave-dominated delta. *Sedimentology* 57: 760-785.
- Clifton, H.E., 2006. A re-examination of facies models for clastic shorelines. In H.W., Posamentier and R.G., Walker (Eds.) *Facies Models Revisited*. SEPM Special Publication 84, p. 293-337.
- Colombera, L. and N.P. Mountney, 2020. On the geological significance of clastic parasequences. *Earth-Science Reviews*, in press.
- Cowell, P.J., P.S. Roy and R.A. Jones, 1995. Simulation of large-scale coastal change using a morphological behavior model. *Marine Geology* 126: 45-61.
- Cummings, D.I., S. Dumas and R.W. Dalrymple, 2009. Fine-grained versus coarse-grained wave ripples generated experimentally under large-scale oscillatory flow. *Journal of Sedimentary Research* 79: 83-93.
- Davidson-Arnott R.G.D., 2010. *Introduction to coastal processes and geomorphology*. Cambridge university press, 442 pp.
- Davidson-Arnott, R.G.D. and B. Greenwood, 1976. Facies relationships on a barred coast, Kouchibouguac Bay, New Brunswick, Canada, in Davis R.A.Jr., and Ethington, R.L., eds., *Beach and Nearshore Sedimentation*. *Society of Economic Paleontologists and Mineralogists Special Publication* 24: 149-168.
- Forzoni, A., G.J. Hampson and J.E.A. Storms, 2015. Along-strike variations in stratigraphic architecture of shallow-marine reservoir analogues: Upper Cretaceous Panther Tongue delta and coeval shoreface, Star Point Sandstone, Wasatch plateau, Central Utah, U.S.A. *Journal of Sedimentary Research* 85: 968-989.
- Gani, M.R. and J.P. Bhattacharya, 2007. Basic Building Blocks and Process Variability of a Cretaceous Delta: Internal Facies Architecture Reveals a More Dynamic Interaction of River, Wave, and Tidal Processes Than Is Indicated by External

- Shape. *Journal of Sedimentary Research* 77: 284-302.
- Gingras, M.K., M.E. Räsänen, S.G. Pemberton and L.P. Romero**, 2002. Ichnology and sedimentology reveal depositional characteristics of bay-margin parasequences in the Miocene Amazonian foreland basin. *Journal of Sedimentary Research* 72: 871-883.
- Graham, G.H., Jackson, M. D. and Hampson, G. J.**, 2015. Three-dimensional modeling of clinoforms in shallow-marine reservoirs: Part 1. Concepts and application. *AAPG Bulletin* 99: 1013-1047.
- Greenwood, B. and Davidson-Arnott, R.G.**, 1979. Sedimentation and equilibrium in wave-formed bars: a review and case study. *Canadian Journal of Earth Science* 16: 312-332.
- Greenwood, B. and P.R. Mittler**, 1985. Vertical sequence and lateral transitions in the facies of a barred nearshore environment. *Journal of Sedimentary Petrology* 55: 366-375.
- Hampson, G.J.**, 2016. Towards a sequence stratigraphic solution set for autogenic processes and allogenic controls: Upper Cretaceous strata, Book Cliffs, Utah, USA. *Journal of Geological Society* 173: 817-836.
- Hampson, G.J.**, 2000. Discontinuity surfaces, clinoforms, and facies architecture in a wave-dominated, shoreface-shelf parasequence. *Journal of Sedimentary Research* 70: 325-340.
- Hampson, G.J. and J.A. Howell**, 2005. Sedimentologic and geomorphic characterization of ancient wave-dominated shorelines: examples from the Late Cretaceous Blackhawk Formation, Book Cliffs, Utah. In Bhattacharya, J.P., and Giosan, L., (eds.) *Deltas Old and New*. SEPM, Special Publication 83: 133-154.
- Hampson, G.J., A.B. Rodriguez, J.E.A. Storms, H.D. Johnson and G.T. Meyer**, 2008. Geomorphology and high-resolution stratigraphy of progradational wave-dominated shoreline deposits: impact on reservoir-scale facies architecture. In Hampson, G.J., Steel, R.J., Burgess, P.M., and Dalrymple, R.W., (eds.) *Recent Advances in Models of Siliciclastic Shallow-Marine Stratigraphy*. SEPM, Special Publication 90: 117-142.
- Hampson, G.J., Gani, M.R., Sahoo, H., Rittersbacher, A., Irfan, N., Ranson, A., Jewell, T.O., Gani, N.D.S., Howell, J.A., Buckley, S.J. and B. Bracken**, 2012. Controls on large-scale patterns of fluvial sandbody distribution in alluvial to coastal plain strata: Upper Cretaceous Blackhawk Formation, Wasatch Plateau, Central Utah, USA. *Sedimentology* 59: 2226-2258.
- Helland-Hansen, W. and O.J. Martinsen**, 1996. Shoreline trajectories and sequences; description of variable depositional-dip scenarios. *Journal of Sedimentary Research* 66: 670-688.
- Heller, P.L., B.A. Burns and M. Marzo**, 1993. Stratigraphic solution sets for determining the roles of sediment supply, subsidence, and sea level on transgressions and regressions. *Geology* 21: 747-750.
- Howell, J.A., E. Schwarz, L.A. Spalletti and G.D. Veiga**, 2005. The Neuquén basin: an overview. In Veiga, G.D., Spalletti, L.A., Howell, J.A., and Schwarz, E., (eds.) *The Neuquén Basin, Argentina: A Case Study in Sequence Stratigraphy and Basin Dynamics*. Geological Society of London, Special Publication 252: 1-14.
- Hughes, M.G., T. Aagaard, T.E. Baldock and H.E. Power**, 2014. Spectral signatures for swash on reflective, intermediate and dissipative beaches. *Marine Geology* 355: 88-97.
- Hunter, R.E., H.E. Clifton and R.L. Phillips**, 1979. Depositional processes, sedimentary structures, and predicted vertical sequences in barred nearshore systems, southern Oregon coast. *Journal of Sedimentary Petrology* 49: 711-726.
- Isla, M.F.**, 2019. Estratigrafía secuencial de alta resolución de las unidades marino someras del Miembro Pilmatué (Formación Agrío) en la Cuenca Neuquina central: procesos, implicancias paleogeográficas y caracterización de reservorios. Tesis Doctoral, Facultad de Ciencias Naturales y Museo, Universidad Nacional de La Plata, 317 pp. (inédito).
- Isla, M.F., E. Schwarz and G.D. Veiga**, 2018. Bedset characterization within a wave-dominated shallow-marine succession: an evolutionary model related to sediment imbalances. *Sedimentary Geology* 374: 36-52.
- Isla, M.F., E. Schwarz and G.D. Veiga**, 2020. The record of a non-barred clastic shoreline. *Geology*, in press.
- Lazo D., M. Cichowolski, D. Rodríguez and M.B. Aguirre-Urreta**, 2005. Lithofacies, palaeoecology and palaeoenvironments of the Agrío Formation, Lower Cretaceous of the Neuquén Basin, Argentina. In Veiga, G.D., Spalletti, L.A., Howell, J.A., and Schwarz, E., (eds.) *The Neuquén Basin, Argentina: A Case Study in Sequence Stratigraphy and Basin Dynamics*. Geological Society of London, Special Publication 252: 295-315.
- Legarreta, L. and M.A. Uliana**, 1991. Jurassic-Cretaceous marine oscillations and geometry of a back-arc basin fill, central Argentine Andes. In MacDonald, D.I.M., (ed.) *Sedimentation, tectonics and eustasy. Sea level changes at active margins*. IAS, Special Publication 12: 429-450.
- Li, L., Walstra, D.J.R. and J.E.A. Storms**, 2015. The impact of wave-induced longshore transport on a delta-shoreface system. *Journal of Sedimentary Research* 85: 6-20.
- Longhitano, S.G. and R.J. Steel**, 2017. Deflection of the progradational axis and asymmetry in tidal seaway and strait deltas: insights from two outcrop case studies. In G.J., Hampson, A.D., Reynolds, B., Kostic and M.R., Well (Eds.) *Sedimentology of paralic reservoirs: recent advances*. Geological Society, London, Special Publications 444: 141-172.
- Maceachern, J.A. and S.G. Pemberton**, 1992. Ichnological aspects of Cretaceous shoreface succession and shoreface variability in the Western Interior Seaway of North America. In Pemberton, S.G., (ed.) *Applications of Ichnology to Petroleum Exploration*. SEPM, Core Workshop 17: 57-84.
- Masselink, G. and J.A. Puleo**, 2006. Swash-zone morphodynamics. *Continental Shelf Research* 26: 661-680.
- Miall, A.D.**, 1985. Architectural-element analysis: a new method of facies analysis applied to fluvial deposits. *Earth-Science Reviews* 22: 261-308.
- Miall, A.D.**, 1988. Architectural elements and bounding surfaces in fluvial deposits: anatomy of the Kayenta Formation (Lower Jurassic), southwest Colorado. *Sedimentary Geology* 55: 233-262.
- Muto, T., R.J. Steel and P.M. Burgess**, 2016. Contributions to sequence stratigraphy from analogue and numerical experiments. *Journal of Geological Society* 173: 837-844.
- Niedoroda, A.W., D.J. Swift, A.G.Jr. Figueiredo and G.L. Freeland**, 1985. Barrier island evolution, middle Atlantic shelf, USA Part II: Evidence from the shelf floor. *Marine Geology* 63: 363-396.
- Ortiz, A.C. and A.D. Ashton**, 2016. Exploring shoreface dynamics and a mechanistic explanation for a morphodynamic depth of closure: *Journal of Geophysical Research. Earth Surface* 121: 442-464.
- Otvos, E.G.**, 2000. Beach ridges—definitions and significance. *Geomorphology* 32: 83-108.

- Pattison, S.A.**, 1995. Sequence stratigraphic significance of sharp-based lowstand shoreface deposits, Kenilworth Member, Book Cliffs, Utah. *AAPG bulletin* 79: 444-462.
- Pellegrini, C., V. Maselli, F. Gamberi, A. Asioli, K.M. Bohacs, T.M. Drexler and F. Trincardi**, 2017. How to make a 350-m-thick lowstand systems tract in 17,000 years: The Late Pleistocene Po River (Italy) lowstand wedge. *Geology* 45: 327-330.
- Plint, A.G.**, 2010. *Facies models 4*. *GEOtext* 6: 167-199.
- Posamentier, H.W. and G.P. Allen**, 1999. Siliciclastic sequence stratigraphy: concepts and applications. *SEPM, Concepts in Sedimentology and Palaeontology* 7, 216 pp.
- Reading, H.G. and J.D. Collinson**, 1996. Clastic Coasts, in Reading, H.G., ed., *Sedimentary Environments: Processes, Facies and Stratigraphy*. Blackwell Science, Oxford, p. 154-231.
- Ridente, D.**, 2016. Releasing the sequence stratigraphy paradigm. Overview and perspectives. *Journal of the Geological Society* 173: 845-853.
- Rodriguez, A.B., J.B. Anderson and A.R. Simms**, 2005. Terrace inundation as an autocyclic mechanism for parasequence formation: Galveston Estuary, Texas, USA. *Journal of Sedimentary Research* 75: 608-620.
- Sagasti, G.**, 2005. Hemipelagic record of orbitally-induced dilution cycles in Lower Cretaceous sediments of the Neuquén Basin. In Veiga, G.D., Spalletti, L.A., Howell, J.A., and Schwarz, E., (eds.) *The Neuquén Basin, Argentina: A Case Study in Sequence Stratigraphy and Basin Dynamics*. Geological Society of London, Special Publication 252: 231-250.
- Schwartz, R.K. and W.A. Birkemeier**, 2004. Sedimentology and morphodynamics of a barrier island shoreface related to engineering concerns, Outer Banks, NC, USA. *Marine Geology* 211: 215-255.
- Schwarz E. and J.A. Howell**, 2005. Sedimentary evolution and depositional architecture of a Lowstand Sequence Set: The Lower Cretaceous Mulichinco Formation, Neuquén Basin, Argentina. In Veiga, G.D., Spalletti, L.A., Howell, J.A., and Schwarz, E., (eds.) *The Neuquén Basin, Argentina: A Case Study in Sequence Stratigraphy and Basin Dynamics*. Geological Society of London, Special Publication 252: 109-138.
- Schwarz, E., G.D. Veiga, G. Álvarez Trentini, M.F. Isla and L.A. Spalletti**, 2018. Expanding the spectrum of shallow-marine, mixed carbonate-siliciclastic systems: processes, facies distribution, and depositional controls of a siliciclastic-dominated example. *Sedimentology* 65: 1558-1589.
- Scotese, C.R.**, 2000. The Paleomap Project: World Wide Web address: <http://www.scotese.com>.
- Sech, R.P., M.D. Jackson and G.J. Hampson**, 2009. Three-dimensional modeling of a shoreface-shelf parasequence reservoir analog: Part 1. Surface-based modeling to capture high-resolution facies architecture. *AAPG Bulletin* 93: 1155-1181.
- Somme, T.O., J.A. Howell, G.J. Hampson, J.E.A. Storms, R.J. Steel, P.M. Burgess and R.W. Dalrymple**, 2008. Genesis, architecture, and numerical modeling of intra-parasequence discontinuity surfaces in wave-dominated deltaic deposits: Upper Cretaceous Sunnyside Member, Blackhawk Formation, Book Cliffs, Utah, USA. In Hampson, G.J., Steel, R.J., Burgess, P.M., and Dalrymple, R.W., eds., *Recent Advances in Models of Siliciclastic Shallow-Marine Stratigraphy*. SEPM, Special Publication 90: 421-441.
- Spalletti L., G.D. Veiga and E. Schwarz**, 2011. La Formación Agrio (Cretácico temprano) en la Cuenca Neuquina. *Relatorio del XVIII Congreso Geológico Argentino*, p. 145-157.
- Storms, J.E.A. and G.J. Hampson**, 2005. Mechanisms for forming discontinuity surfaces within shoreface-shelf parasequences: sea level, sediment supply, or wave regime?. *Journal of Sedimentary Research* 75: 67-81.
- Swift, D.J.**, 1975. Barrier-island genesis: evidence from the central Atlantic shelf, eastern USA. *Sedimentary Geology* 14: 1-43.
- Swift, D.J., B.S. Parsons, A. Foyle and G.F. Oertel**, 2003. Between beds and sequences: stratigraphic organization at intermediate scales in the Quaternary of the Virginia coast, USA. *Sedimentology* 50: 81-111.
- Tamura, T.**, 2012. Beach ridges and prograded beach deposits as palaeoenvironment records. *Earth-Science Reviews* 114: 279-297.
- Van Wagoner, J.C., R.M.J. Mitchum, K.M. Campion and V.D. Rahmanian**, 1990. Siliciclastic Sequence Stratigraphy in Well Logs, Cores, and Outcrop: Concepts for High-Resolution Correlation of Time and Facies. *AAPG Methods in Exploration* 7: 55 pp.
- Van Wagoner, J.C., H.W. Posamentier, R.M.J. Mitchum, P.R. Vail, J.F. Sarg, T.S. Loutit and J. Hardenbol**, 1988. An overview of the fundamentals of sequence stratigraphy and key definitions. In Wilgus, C.K., Hastings, B.S., Kendall, C.G.S.C., Posamentier, H.W., Ross, C.A., and Van Wagoner, J.C., eds., *Sea-Level Changes: an Integrated Approach*. Society of Economic Paleontologists and Mineralogists 42: 39-45.
- Veiga, G.D., L.A. Spalletti and S.S. Flint**, 2007. Anatomy of fluvial lowland wedge: the Avilé member of the Agrio Formation (Hauterivian) in central Neuquén Basin (northwest Neuquén Province), Argentina. In Nichols, G., Williams, E., and Paola, C., eds., *Sedimentary Processes, Environments and Basins, A tribute to Peter Friend*. IAS, Special Publication 38: 341-365.
- Vergani, G.D., Tankard, A.J., Belotti, H.J. and H.J. Welsink**, 1995. Tectonic evolution and paleogeography of the Neuquén Basin, Argentina. In: Tankard, A.J., Suarez Soruco, R., and Welsink, H.J., eds., *Petroleum Basins of South America*. AAPG Memoirs 62: 383-402.
- Wijnberg, K.N. and A. Kroon**, 2002. Barred beaches. *Geomorphology* 48: 103-120.
- Wright, L.D. and A.D. Short**, 1984. Morphodynamic variability of surf zones and beaches: A synthesis. *Marine Geology* 56: 93-118.
- Wright, L.D., J.D. Boon, S.C. Kim and J.H. List**, 1991. Modes of cross-shore sediment transport on the shoreface of the Middle Atlantic Bight. *Marine Geology* 96: 19-51.
- Zecchin, M., M. Caffau, O. Catuneanu and D. Lenaz**, 2017. Discrimination between wave-ravinement surfaces and bedset boundaries in Pliocene shallow-marine deposits, Croton Basin, southern Italy: An integrated sedimentological, micropalaeontological and mineralogical approach. *Sedimentology* 64: 1755-1791.
- Zecchin, M. and O. Catuneanu**, 2013. High-resolution sequence stratigraphy of clastic shelves I: Units and bounding surfaces. *Marine and Petroleum Geology* 39: 1-25.
- Zhang, Y., D.J.P. Swift, A.W. Nedoroda, C.W. Reid and J.A. Thorne**, 1997. Simulation of sedimentary facies on the northern California shelf: implications for an analytical theory of facies differentiation. *Geology* 27: 635-638.